Agricultural and Forest Meteorology 300 (2021) 108309

Contents lists available at ScienceDirect

Agricultural and Forest Meteorology

journal homepage: www.elsevier.com/locate/agrformet

Agricultural and Forest Meteorology

Biophysical drivers of net ecosystem and methane exchange across phenological phases in a tidal salt marsh

Alma Vázquez-Lule, Rodrigo Vargas *

Department of Plant and Soil Sciences, University of Delaware, Newark, DE, USA

ARTICLE INFO

Keywords:
maturity
dormancy
eddy covariance
gap-filling
carbon source
warming potential

ABSTRACT

Salt marshes are large carbon reservoirs as part of blue carbon ecosystems. Unfortunately, there is limited information about the net ecosystem (NEE) and methane (CH_4) exchange between salt marshes and the atmosphere to fully understand their carbon dynamics. We tested the influence of biophysical drivers by plant phenological phases (i.e., Greenup, Maturity, Senescence and Dormancy) on NEE and CH_4 exchange in a grass-dominated temperate tidal salt marsh. We used three years of data derived from eddy covariance, PhenoCam (to measure vegetation phenology), and ancillary meteorological and water/soil variables. Overall, NEE showed significant differences among all phenological phases ($p < 0.05$), while CH_4 exchange had significant differences among all phases except for Greenup and Dormancy. Net CO_2 uptake was higher across Maturity (-61 g C-CO_2 m^2), while CO_2 emissions were higher during Dormancy (182 g C-CO_2 m^2). The lower but constant CO_2 emissions during Dormancy overshadowed the CO_2 uptake during the growing season and contributed to >72% of the annual CO_2 emissions in this ecosystem. Net CH_4 emissions were higher during Maturity (3.7 g C-CH_4 m^2) and Senescence (4.2 g C-CH_4 m^2). Photosynthetically active radiation (PAR) substantially influenced ($r^2 > 0.57$) daytime NEE across phenological phases, but a combination of variables including water table level (WTL), water temperature and atmospheric pressure were relevant to explain CH_4 exchange. The study site was an overall net carbon source to the atmosphere with annual emissions of 13-201 g C-CO_2 $m^{-2}yr^{-1}$ and 8.5-15.2 g C-CH_4 $m^{-2}yr^{-1}$. Our findings provide insights on: a) the role of plant phenological phases on ecosystem-scale CO_2 and CH_4 fluxes; b) challenges for modeling ecosystem-scale CO_2 and CH_4 fluxes in salt marshes; and c) the potential net loss of carbon to the atmosphere that should be considered for carbon management and accounting in these ecosystems.

1. Introduction

Salt marshes are one of the most productive ecosystems with the capacity to sequester atmospheric carbon dioxide (CO_2) into plant biomass and to trap and bury carbon in their sediments from autochthonous and allochthonous sources (i.e., *Blue carbon*; (McLeod et al., 2011; Van de Broek et al., 2018)). This carbon could potentially remain in the ecosystem for thousands of years (Gedan et al., 2009), be laterally exported via water exchange with the coastal ocean (Bauer et al., 2013; Wang et al., 2017; Trifunovic et al., 2020), or vertically exchanged with the atmosphere as CO_2 and methane (CH_4) fluxes ((Forbrich and Giblin, 2015); Holm et al., 2016; Kathilankal et al., 2008; Knox et al., 2018; Krauss et al., 2016; (Li et al., 2018)). Unfortunately, there is limited information from most of these fluxes that hampers our understanding of the role of salt marsh ecosystems in the local-to-global carbon budget (Bauer et al., 2013; Bridgham et al., 2006; Hayes et al., 2018; McNicol et al., 2017).

Salt tolerant perennial grasses are the dominant vegetation in salt marsh ecosystems of the Mid-Atlantic region (Crosby et al., 2015; Vasquez et al., 2006) with high turnover rates during a yearly cycle and with defined phenological phases (Ghosh and Mishra, 2017). These phases are influenced by changes in temperature and photoperiod that could influence carbon dynamics by directly regulating plant photosynthesis activity, ecosystem respiration and carbon allocation (Crosby et al., 2016, 2015; Ghosh and Mishra, 2017; Kirwan et al., 2009; Piao et al., 2015; Richardson et al., 2010). Consequently, it is important to understand how carbon dynamics respond to different plant phenological phases to improve process-based models in these ecosystems (Tang et al., 2016; Walter and Heimann, 2000).

The relationship between carbon dynamics and plant phenology in salt marshes has been explored at the hourly scale (Diefenderfer et al., 2018), monthly scale (Guo et al., 2009; Holm et al., 2016; Zhong et al.,

* Corresponding author.
E-mail address: rvargas@udel.edu (R. Vargas).

https://doi.org/10.1016/j.agrformet.2020.108309
Received 26 June 2020; Received in revised form 22 December 2020; Accepted 24 December 2020
Available online 12 January 2021

2016), within seasons (i.e. spring, summer and winter; (Artigas et al., 2015; Schäfer et al., 2014) and growth stages of vegetation (i.e., fast, middle and terminal; Chu et al., 2018). However, specific phenological phases associated with plant metabolism such as Greenup, Maturity, Senescence and Dormancy following standardized protocols (Filippa et al., 2016; Kim et al., 2018; Zhang et al., 2005) have not been widely used (O'Connell et al., 2020; Trifunovic et al., 2020). Digital repeated photography (i.e., PhenoCam) is an alternative cost-effective near-surface remote sensing tool to monitor changes in canopy phenology (Richardson et al., 2009). These data can be synchronized with ecosystem-scale measurements of carbon exchange between the land surface and the atmosphere to represent and model ecosystem productivity (Knox et al., 2017; Migliavacca et al., 2011; Toomey et al., 2015).

Salt marshes represent ecosystems within the aquatic-terrestrial interface, and consequently tidal patterns and water table level (WTL) can influence carbon dynamics. Previous studies have found that tidal patterns in these ecosystems influence land-atmosphere CO_2 dynamics where an increase of CO_2 uptake was observed with medium-to-high tides (Schäfer et al., 2014; Guo et al., 2009; Knox et al., 2018), or a decrease of CO_2 uptake with high tides (Forbrich and Giblin, 2015; Kathilankal et al., 2008). These responses are dependent on site-specific biochemical conditions (Capooci et al., 2019; Seyfferth et al., 2020), the interaction of plant species with flooding conditions (Kathilankal et al., 2008), as well as plant distribution across the landscape (e.g., low or high marshes; (Artigas et al., 2015; Forbrich and Giblin, 2015)).

Most of our understanding of carbon dynamics in salt marshes is based on CO_2 dynamics but CH_4 dynamics are still a science frontier. Previous studies reported that CH_4 emissions increased in freshwater wetlands with air temperature and high water table level (H-WTL), as these conditions favor anaerobic metabolism in soils that may enhance methanogenesis (Holm et al., 2016; Krauss et al., 2016). In contrast, other studies in salt marshes showed a decrease in CH_4 emissions with water surges (Diefenderfer et al., 2018). In coastal wetlands, the increase of WTL could influence salinity concentrations that also influence CH_4 fluxes through different biophysical mechanisms (Capooci et al., 2019; Poffenbarger et al., 2011; Seyfferth et al., 2020). Furthermore, other studies have reported that CH_4 fluxes could be influenced by changes in atmospheric pressure (Rey-Sanchez et al., 2018; Sturtevant et al., 2016), air turbulence (Chu, 2014; Rey-Sanchez et al., 2018), or water flux and plant-mediated transport (Morin, 2019; Morin et al., 2014). Consequently, much more information is needed to identify the biophysical drivers of CH_4 fluxes in these ecosystems to properly represent them in process-based models.

In this study, we used the eddy covariance technique (EC) to measure the mass and energy exchange between a grass-dominated temperate salt marsh and the atmosphere. The EC calculates the vertical flux density of mass and energy by the covariance of turbulent fluctuations of vertical wind velocity and the scalar of interest (i.e., CO_2, CH_4, water vapor flux; Foken et al., 2012). This approach was first used in salt marshes to quantify energy and CO_2 exchange by Kathilankal et al., (2008), but nearly 23 studies now report the use of EC. Over 85% of those studies have focused on CO_2 dynamics, and <15% reported CO_2 and CH_4 dynamics (Table 1 Supporting Information). Consequently, much more information is needed to couple CO_2 and CH_4 dynamics for local-to-global studies and provide insights and benchmarks for process-based models and synthesis studies (Knox et al., 2019).

Our overarching goal was to describe the influence of plant phenological phases (i.e., Greenup, Maturity, Senescence and Dormancy) on the ecosystem exchange of CO_2 and CH_4 in a temperate tidal salt marsh within the mid-Atlantic coast. We further identify the key biophysical drivers (i.e., climatic, atmospheric, soil and water) that regulate the net ecosystem exchange (NEE) and CH_4 exchange across those phenological phases, daytime/nighttime and different WTL. We asked three interrelated research questions with associated hypotheses:

Table 1
Biophysical drivers selected for statistical analyses and functional relationships with NEE and CH_4 exchange.

Biophysical Driver	Abbreviation	Units	Type of wetland
Atmospheric Pressure	PA	kPa	freshwater wetland#[14]
Relative Humidity	RH	%	salt marsh*[8]
Air Temperature	TA	°C	brackish tidal marsh*[1], salt marsh**[2], salt marsh*[3], brackish and freshwater marshes#[5,13], salt marsh*[6], salt marsh*[8]
Incoming Photosynthetic Active Radiation	PAR	μmol Photon m^{-2} s^{-1}	brackish tidal marsh*[1], salt marsh**[2], mangrove and freshwater marsh*[4], salt marsh*[6]
Soil Temperature	TS	°C	brackish tidal marsh*[1], brackish and freshwater marshes#[5], freshwater wetland#[14], estuarine wetland#[15]
Water Table Level	WTL	m	brackish tidal marsh*[1], salt marsh**[2], salt marsh*[3], brackish and freshwater marshes#[5,13], salt marsh*[7], salt marsh*[9], salt marsh*[10] freshwater wetland#[14]
Friction Velocity (u.)	USTAR	m s^{-1}	estuarine wetland#[15]
Wind Direction	WD	°	salt marsh*[8], freshwater wetland#[14]
Water Temperature	TW	°C	salt marsh*[3], brackish and freshwater marshes#[5], estuarine wetland#[11], coastal petland#[12]
Dissolve Oxygen in Water	DO	mg l^{-1}	salt marsh**[16]
Salinity in Water	SAL	ppt	brackish tidal marsh*[1], salt marsh*[3], brackish and freshwater marshes#[5,13]
H_2O exchange	fH2O	mmolH_2O mol^{-1}	freshwater wetland#[14]

Notes:
Flux measured: *NEE (Net Ecosystem Exchange); ** CH_4; #Synchronized measurements of NEE and CH_4.
[1] Knox et al., 2018.
[2] Li et al., 2018.
[3] Jia et al., 2017.
[4] Malone et al., 2016.
[5] Krauss et al., 2016.
[6] Zhong et al., 2016.
[7] Forbrich and Giblin, 2015.
[8] Artigas et al., 2015.
[9] Guo et al., 2009.
[10] Kathilankal et al., 2008.
[11] Rey-Sanchez et al., 2018.
[12] Windham-Myers et al., 2018.
[13] Holm et al., 2016.
[14] Sturtevant, et al., 2016.
[15] Chu et al., 2014.
[16] Al-Haj and Fulweiler, 2020. References indicate studies that have identified each driver as relevant for a study site.

(a) How do changes in plant phenology influence NEE and CH_4 exchange in a grass-dominated temperate tidal salt marsh? We hypothesized that net CO_2 uptake will increase during the Maturity phase due to an increase of photosynthesis activity, that will be higher than potential ecosystem respiration (Artigas et al., 2015; Chu, 2014; Schäfer et al., 2014; Tonti et al., 2018). We hypothesized that net CH_4 emissions will increase during the Maturity phase as well, due to the peak of growth in vegetation and its potential mediated-effect on CH_4 transport from soils to

the atmosphere (Kludze and Delaune, 1994; Morin et al., 2014). We also expected net CH_4 emissions during Senescence due to a potential increase of labile organic matter on soils available for decomposition and methanogenesis (Chanton et al., 2002; Chu, 2014; Seyfferth et al., 2020; Whiting and Chanton, 1993; Zhang and Ding, 2011).

(b) How does WTL (i.e., Low water table level, L-WTL: at and below soil surface, and High water table level, H-WTL: above soil surface) influence NEE and CH_4 exchange? We hypothesized that net CO_2 emissions will be reduced when WTL reach higher values, due to lower diffusion rates in water (Knox et al., 2018; Schäfer et al., 2014). In addition, we expected a decrease on net CO_2 uptake by suppression or reduction of canopy photosynthesis due to flooding conditions (Forbrich and Giblin, 2015; Guo et al., 2009; Kathilankal et al., 2008). For CH_4 exchange, we also expected a decrease in CH_4 emissions due to a potential increase in salinity with H-WTL and consequently, its negative effect on methanogenesis (Capooci et al., 2019; Krauss et al., 2016; Li et al., 2018; Neubauer et al., 2013).

(c) What are the most relevant biophysical drivers that influence NEE and CH_4 exchange during daytime and nighttime across phenological phases? We hypothesized that biophysical drivers that regulate photosynthesis activity in terrestrial ecosystems, such as light availability and temperature, will also regulate daytime NEE when vegetation is active (Artigas et al., 2015; Schäfer et al., 2014; Zhong et al., 2016). We expected that the increase of temperature among the phenological phases might regulate NEE nighttime (i.e., net nighttime CO_2 emissions), mainly due to an increase of soil heterotrophic metabolism and belowground plant respiration. In contrast, we hypothesized that changes on WTL will regulate CH_4 exchange due to its influence on soil biogeochemical processes (via changes in redox conditions) that are responsible of anaerobic decomposition of organic matter and CH_4 production (Seyfferth et al., 2020).

2. Materials and methods

2.1. Site description

The study site is the St. Jones Reserve, Delaware, USA (39°05' 17.49", 75°26'14.00"). It is a temperate tidal salt marsh at the Mid-Atlantic region, characterized with high productivity, medium seasonality and with the peak of phenology during summer (Villarreal et al., 2018). It is part of the Delaware National Estuarine Research Reserve and one of the National Estuarine Reserve Research System (NERRS) from the National Oceanic and Atmospheric Administration. It is also part of the AmeriFlux Network (US-StJ, St Jones Reserve; (Vázquez-Lule and Vargas, 2015)) and PhenoCam Network (stjones; Seyednasrollah et al., 2019) since 2015.

The salt marsh area is heterogeneous and characterized by low and high marshes (Correll et al., 2019). The most dominant plant species is *Spartina alterniflora* (= *Sporobolus alterniflorus* (Loisel.); Peterson et al., 2014) covering ~66% of the salt marsh area, followed by *Spartina cynosuroides* (i.e., ~29%) (= *Sporobolus cynosuroides* (L.); Peterson et al., 2014) and *Phragmatis australis* (i.e., <5%). Soils are silty clay loam (10% sand, 61% silt and 29% clay; Capooci et al., 2019), with an average dry bulk density of 0.43, soil organic carbon of 9%, and organic matter of 21.5%. Tides are semidiurnal, with two similar equal high tides and low tides in a period of 24 hours (CEC, 2015).

2.2. Eddy covariance and meteorological measurements

An EC tower (height of 3.5 m) was established during the Spring of 2015. It is equipped with a WindMaster Pro anemometer, model 160724 (Gill Instruments, Lymington, Hamisphere, UK), a LI-7200RS enclosed path CO_2/H_2O Analyzer and a LI-7700 open path CH_4 analyzer (LI-COR Environmental, Lincoln, NE, USA). Ancillary measurements include an air temperature and relative humidity (Probe HMP155, Vaisala, Helsinki, Finland), net radiation (CNR4 Net Radiometer, Kipp & Zonen B.V., Delft, The Netherlands), Photosynthetically Active Radiation (PAR) (Li-190SL, LI-COR Environmental, Lincoln, NE, USA) and soil temperature at 10 cm of depth (ML2x Theta Soil Moisture Probe, Delta-T Devices, Cambridge, UK).

A PhenoCam was installed in September 2015 (StarDot NetCam SC; StarDot Technologies, California, USA) and has collected continuous photographs in Red-Green-Blue and InfraRed every 30 min. Salt marsh vegetation represented ~ 80% of the camera's field range. Auxiliary water parameters (i.e., WTL, water temperature, dissolve oxygen and salinity) were measured within a YSI 6600 sonde (YSI Inc.,Yellow Springs, OH, USA) installed in a nearby creek within the EC footprint. Data were collected at 15 min intervals by NEERSS and QA/QC was evaluated under the NERR System-wide Monitoring Program, following the Centralized Data Management standardized protocol (NOAA National Estuarine Research Reserve, 2015).

2.3. Eddy covariance quality control and flux calculation

We used EC data collected from April 2015 to December 2017. We followed a standard protocol to process the data until level L2A of the AmeriFlux network (AmeriFlux and U. S. Department of Energy, 2020). The EC raw data was processed using EddyPro 6.2.0 (LI-COR Environmental, Lincoln, NE, USA). We applied: a) coordinate double rotation for potential misalignments of the anemometer respect to the local wind streamlines; b) block average based in Reynolds decomposition to correct the turbulence fluctuations, c) and when needed, the Webb-Pearman-Leuning correction for air density fluctuations if the reading of the internal thermopars of the LI-7200RS were missing (i.e., thermopar malfunction was less than 4% of the fluxes during the study period). We used (Kljun et al., 2004) to estimate the fetch and the climatology footprint and applied the statistical tests of Vickers and Mahrt (1997) to despike data. We used Moncrieff et al. (2004) for the spectral corrections of low frequency turbulence, and Moncrieff et al. (1997) for high frequency turbulence corrections.

We removed fluxes when sensors registered poor quality of measurements (i.e., fluxes that should be discarded form the dataset with labels of "2"; (Mauder and Foken, 2006), and we kept fluxes with probabilities > 50% inside of the EC footprint. Sixty-six percent of the EC footprint was dominated by *S. alterniflora,* 29% by *S. cynosuroides*, 3% from creeks and the rest from other land covers (i.e., *Phragmites australis*, mudflats and terrestrial border). We set a friction velocity threshold (u*) of 0.068 m/s to remove nighttime low turbulent fluxes, as a standardized processing to reduce the uncertainty during periods with low atmosphere mixing (Papale et al., 2006). To do this, instead of using temperature classes, we used the phenological phases defined for every year (see Section 2.4), and we identified the u* as the median value of the 12 phenological phases for the study period. Overall, for the three years of data we kept ~57% of CO_2 fluxes and ~ 53% of CH_4 fluxes.

2.4. Identifying phenological phases for the canopy

We identified different phenological phases in the salt marsh from January 2015 to December 2017 using the Phenopix R package (Filippa et al., 2016). First, we defined a region of interest inside the camera field range representing the canopy of *S. alterniflora* and *S. cynosuroides*. Second, we calculated the Greenness Index (GI) as the ratio of green digital numbers and the total digital numbers of all color channel information (Red + Green + Blue). We used the function "autoFilter" and the spline filter to estimate daily GI (Migliavacca et al., 2011). GI index before September 2015 was estimated as the average of GI from 2016 and 2017. We used the function of "greenExplore" to fit phenology GI curves for every year and we defined the phenological phases with the "gu" method (Gu et al., 2009). Finally, we defined four phenological

phases: *(a)* Greenup (i.e., April to June), when grasses start to grow, *(b)* Maturity (i.e., July to September), when grasses reach the peak of growth and greenness, *(c)* Senescence (i.e., September to October), when grasses start to decrease in greenness, and *(d)* Dormancy (i.e., November to March), when grasses are inactive.

2.5. Statistical analyses

Our analyzes were based on 30 minutes averages of data from NEE, CH_4 exchange and independent biophysical drivers (Table 1). Data was classified by phenological phase, and daytime (PAR > 0) or nighttime (PAR = 0). We identified significant differences between NEE and CH_4 exchange across years and phenological phases using least square means and adjusting the *p*-values with the Tukey method. This was done using the "emmeans" R package (Lenth et al., 2020).

Average and standard deviation for NEE, CH_4 exchange and biophysical drivers were estimated for daytime, nighttime, phenological phases and WTL. We defined low water table level (L-WTL) when water table was at the soil surface or lower (i.e., negative values), and high water table level (H-WTL) when water table was higher than the soil surface (i.e., positive values). We applied linear regression models to identify relationship between NEE and CH_4 exchange across phenological phases and L-WTL and H-WTL.

We used Canonical Correlation Analyses (CCA) to evaluate the covariance and interaction between NEE and CH_4 exchange with independent drivers (Table 1). CCA is a multivariate correlation analysis that identifies the maximum correlation between matrixes of variables. This analysis is appropriate when there are multiple intercorrelated variables that may explain a dependent variables (Hardoon and Shawe-Taylor, 2004; Mäkelä et al., 2020), such as the case of NEE and CH_4 exchange where more than a single factor influence the fluxes (Knox et al., 2018; Sturtevant et al., 2016; Trifunovic et al., 2020). The CCA method considers a set of dependent variables (i.e., NEE and CH_4 exchange) and a set of independent variables (i.e., biophysical drivers). It calculates eigenvalues matrices from both sets, then it executes all the possible linear combinations to maximize the shared covariance between them. Shared covariance is explained by canonical correlations of every variable in the dependent set and the variance of every variable in the independent set. Canonical correlations and the covariance between variables are expressed as regular correlation coefficients (Thompson, 1984). We did 10 CCA models using the "CCA" R package (González et al., 2008). All models were statistically significant ($p < 0.001$), and we showed results where the correlation coefficient was $\geq |0.4|$. Finally, we showed functional relationships for NEE and CH_4 exchange with drivers using linear regressions.

2.6. Gap-filling, global warming potential and sustained-flux global warming potential

We gap filled NEE and CH_4 exchange only to report annual carbon budgets and the overall global warming potential (GWP) and the sustained-flux global warming potential (SGWP). We did an ensemble of the marginal distribution sampling technique (MDS) and artificial neural nets via deep learning (ANNvDL). The ANNvDL method was only used to gap fill values that were not predicted by the MDS approach (see below). First, we used "ReddyProc" R package (Wutzler et al., 2018) to gap fill NEE and CH_4 exchange for all data in 2015 and 2017, and from April to December 2016. We selected global radiation, soil temperature, air temperature, water dissolve oxygen and water flux as covariables of NEE, and for CH_4 exchange the same variables, but instead of global radiation, we used WTL, as this is an important variable controlling this flux in wetlands (Capooci et al., 2019; Holm et al., 2016; Neubauer et al., 2013). Second, ANNvDL was only used to gap fill NEE and CH_4 exchange data from January to March 2016 using the "keras" library on "TensorFlow" in R package. We selected the following independent variables to predict NEE: TS, TA, PAR, TW, DO, day of the year (DOY), hour. We selected the following independent variables to predict CH_4 exchange: NEE-gap filled, TW, WTL, DO, TA, TS, PA, fH2O, latent and heat fluxes, phenological phases, DOY and hour. The selection of these independent variables was informed from the CCA results and using findings reported by Kim et al., (2020).

We calculated the GWP and the SGWP of NEE and CH_4 exchange for the 20- and 100-year scenarios. Cumulative daily sums of NEE and CH_4 exchange were converted to g m^{-2}, and then we multiplied them times 1 for NEE for both metrics, and times 87 and 96 for CH_4 exchange to consider 20- year scenario for GWP and SGWP respectively, and times 32 and 45 to consider 100-year scenarios for the GWP and SGWP respectively (Neubauer and Megonigal, 2019). We report the mean GWP and SGWP as CO_2 equivalents ($CO_{2\text{-eq}}$) by phenological phases and scenario. Detailed information by phenological phases and year is in Table 2 and 3 of Supporting Information.

3. Results

3.1. Phenology and General Climatology

Greenup and Dormancy were the most consistent phenological phases in terms of when they started and their length. Greenup started around April 19 and had an average length of 77 ±8 days, Maturity around July 5 with an average length of 60 ±28 days, Senescence around September 3 with an average length of 60 ±28 days, while Dormancy started around November 3 and it continued until the next Greenup phase, with an average length of 168 ±3 days (Fig. 1a).

During the study period, we found a mean annual air temperature of 14°C, with an average daily maximum in July of 25°C, an average daily minimum in January of 1°C (Fig. 1b), and a mean annual precipitation of 576 mm yr^{-1} (Fig. 1c). Prevalent wind directions (~80%) were from Southwest and Southeast, with a maximum daily mean wind speed of 12.2 m s^{-1} and an average daily mean wind speed of 2.13 m s^{-1}. Mean daily tidal range was 83 cm, with a maximum mean daily tide of 221 cm and minimum mean daily tide of -0.30 cm. Average daily WTL was -0.26 cm with a maximum of 0.52 cm and a minimum of -0.59 cm (Fig. 1c).

3.2. Carbon fluxes and biophysical drivers

This salt marsh had an average NEE of -0.66 (μmol CO_2 m^{-2} s^{-1}), with a standard deviation of ±8.30 (μmol CO_2 m^{-2} s^{-1}), while CH_4 exchange had an average of 34.16 (nmol CH_4 m^{-2} s^{-1}) with a standard deviation of ± 60.23 (nmol CH_4 m^{-2} s^{-1}; Fig. 2). Higher CO_2 uptake happened across Maturity (-1.94 ±11.93 μmol CO_2 m^{-2} s^{-1}; Fig. 2b), and higher CO_2 emissions at Dormancy (1.11 ±2.35 μmol CO_2 m^{-2} s^{-1}; Fig. 2d). Release of CH_4 was higher across Maturity (58.03 ±80.81 nmol CH_4 m^{-2} s^{-1}; Fig. 2f) and Senescence (69.39 ±120.87 nmol CH_4 m^{-2} s^{-1}; Fig. 2g), and lower during Greenup (15.66 ±19.89 nmol CH_4 m^{-2} s^{-1}; Fig. 2e) and Dormancy (15.66 ±48.96 nmol CH_4 m^{-2} s^{-1}; Fig. 2h). We found no significant differences in the annual means across years for NEE and CH_4 exchange. NEE showed significant differences among all phenological phases ($p < 0.05$), while CH_4 exchange had significant differences among all phases except for Greenup and Dormancy (Fig. 2e and 2h). NEE and CH_4 exchange showed a higher relationship between them during nighttime ($r > 0.30$; Fig. 3k-t) than during daytime ($0.19 < r$ Fig. 3a-j), with no significant differences across water table levels. Daytime mean values for NEE and CH_4 exchange showed significant differences between H-WTL and L-WTL for almost all phenological phases ($p < 0.05$; Table 2). CO_2 uptake was larger during H-WTL and across Maturity. In contrast, daytime CH_4 emissions increased with L-WTL across Maturity and Senescence (Table 2). Nighttime mean values for NEE and CH_4 exchange showed significant differences between WTL for all phenological phases ($p < 0.05$; Table 3), except during Dormancy. Nighttime NEE and nighttime CH_4 exchange had an increase on emissions under L-WTL. Nighttime CO_2 emissions were higher during Maturity, and nighttime CH_4 emissions during Maturity and Senescence

Table 2
Daytime mean values for NEE, CH_4 exchange and biophysical drivers across phenological phases and water table levels.

Season	WTL#	NEE(μmol CO_2 m^{-2} s^{-1})	CH4(nmol CH_4 m^{-2} s^{-1})	PAR(μmol photon m^{-2} s^{1})	PA(kPa)	TA(°C)	RH(%)	TS(°C)	TW (°C)	USTAR(m s^{-1})	WD(°)	fH2O(mmolH_2O mol^{-1})	WTL (m)	DO(mg l^{-1})	SAL(ppt)
All phases	L	**-3.82*** ± 8.47	**36.33*** ± 64.76	**624.76** ± 521.64	**101.79*** ± 0.69	**19.93** ± 8.27	**68.71*** ± 19.06	**17.73** ± 5.85	**19.10** ± 7.50	**0.36** ± 0.16	**181.83*** ± 104.73	**16.68*** ± 8.0	**-0.42*** ± 0.29	**3.88*** ± 2.57	**10.39*** ± 4.34
	H	**-4.48*** ± 7.86	**23.11*** ± 51.04	**624.26** ± 484.25	**101.94*** ± 0.69	**19.56** ± 7.36	**69.76*** ± 17.34	**17.53** ± 5.20	**18.99** ± 6.80	**0.36** ± 0.15	**160.18*** ± 107.75	**16.14*** ± 7.07	**-0.14*** ± 0.10	**5.26*** ± 2.31	**15.11*** ± 5.28
Greenup	L	**-5.24** ± 9.20	**17.32*** ± 46.62	**746.61*** ± 587.87	**101.52*** ± 0.59	**22.43*** ± 5.60	**68.06*** ± 20.49	**19.17** ± 4.20	**21.86** ± 3.83	**0.38** ± 0.16	**186.26*** ± 89.29	**17.92** ± 5.65	**-0.40*** ± 0.29	**3.81*** ± 2.12	**8.57*** ± 3.48
	H	**-5.56** ± 9.50	**11.25*** ± 44.55	**672.05*** ± 582.82	**101.59*** ± 0.54	**21.33*** ± 4.98	**75.22*** ± 19.74	**18.79** ± 3.51	**22.13** ± 3.76	**0.38** ± 0.16	**153.32*** ± 78.94	**18.49** ± 5.49	**0.09*** ± 0.06	**4.29*** ± 1.55	**12.71*** ± 4.60
Maturity	L	**-7.10*** ± 10.74	**50.78*** ± 64.98	**775.64** ± 558.18	**101.67*** ± 0.46	**26.63*** ± 3.93	**72.03*** ± 15.54	**22*** ± 3.25	**26.21** ± 2.70	**0.33** ± 0.14	**167.66*** ± 99.15	**24.12** *± 5.00	**-0.41*** ± 0.29	**2.66*** ± 2.12	**13.67*** ± 3.76
	H	**-8.19*** ± 10.37	**26.04*** ± 44.48	**751.46** ± 558.37	**101.74*** ± 0.42	**25.78*** ± 3.60	**69.16*** ± 14.33	**21.24*** ± 2.94	**26.25** ± 2.40	**0.33** ± 0.13	**145.19*** ± 98.13	**22*** ± 5.03	**0.11*** ± 0.07	**3.70*** ± 1.48	**18.15*** ± 3.98
Senescence	L	**-2.62*** ± 6.33	**60.51*** ± 80.81	**557.54*** ± 433.55	**101.99*** ± 0.64	**19.55*** ± 5.02	**68.57** ± 18.56	**17.92** ± 4.06	**18.32*** ± 3.72	**0.35*** ± 0.15	**166.51** ± 114.44	**15.40*** ± 6.00	**-0.43*** ± 0.29	**3.24*** ± 1.81	**10.09*** ± 4.05
	H	**-4.27*** ± 5.81	**36.74*** ± 58.93	**634.89*** ± 416.87	**102.09*** ± 0.64	**20.21*** ± 5.03	**68.43** ± 16.53	**18.19** ± 4.04	**18.90*** ± 3.32	**0.38*** ± 0.14	**157.29** ± 116.46	**15.90*** ± 5.78	**0.17*** ± 0.11	**5.06*** ± 1.47	**14.56*** ± 5.63
Dormancy	L	**0.43*** ± 1.68	**12.79*** ± 44.94	**385.20*** ± 362.59	**102.03*** ± 0.89	**9.53*** ± 6.74	**65.39*** ± 21.24	**10.84*** ± 5.12	**8.35*** ± 4.02	**0.37** ± 0.17	**210.59*** ± 109.01	**7.57*** ± 4.34	**-0.45*** ± 0.29	**6.12*** ± 2.72	**8.50*** ± 3.71
	H	**-0.09*** ± 1.84	**6.16** * ± 40.48	**437.41*** ± 352.17	**102.18*** ± 0.91	**10.61*** ± 6.32	**68.84*** ± 19.10	**11.61*** ± 4.75	**9.17*** ± 3.57	**0.37** ± 0.16	**185.64*** ± 115.65	**8.59*** ± 4.30	**0.16*** ± 0.10	**7.93*** ± 2.31	**14.32*** ± 4.96

L: Low water table level; H: High water table level.
*Significant differences ($p < 0.05$).

Table 3
Nighttime mean values for NEE, CH_4 exchange and biophysical drivers across phenological phases and water table levels.

Season	WTL#	NEE (μmol CO_2 m^{-2} s^{-1})	CH4 (nmol CH_4 m^{-2} s^{-1})	PA(kPa)	TA(°C)	RH(%)	TS(°C)	TW (°C)	USTAR (m s^{-1})	WD(°)	fH2O (mmolH_2O mol^{-1})	WTL (m)	DO (mg l^{-1})	SAL (ppt)
All phases	L	**4.93** ± 4.59	**43.39*** ± 62.79	**101.83** ± 0.73	**14.39*** ± 8.20	**81.77*** ± 15.51	**13.92*** ± 5.74	**16.79*** ± 7.67	**0.24** ± 0.14	**189.42*** ± 103.14	**14.78*** ± 8.28	**-0.43*** ± 0.29	**3.61*** ± 2.31	**10.36*** ± 4.47
	H	**4.84** ± 4.12	**26.50*** ± 48.33	**101.83** ± 0.67	**17.08*** ± 6.13	**85.44*** ± 11.96	**15.74*** ± 4.34	**20.26*** ± 6.42	**0.24** ± 0.13	**177.25*** ± 109.49	**17.14*** ± 6.74	**0.15*** ± 0.10	**5.51*** ± 2.08	**16.21*** ± 5.60
Greenup	L	**7.41*** ± 4.48	**27.14*** ± 46.41	**101.46** ± 0.59	**18.77*** ± 4.58	**83.64*** ± 14.11	**16.84*** ± 3.54	**21.38** ± 3.68	**0.25** ± 0.14	**199.62*** ± 81.12	**18.49*** ± 6.00	**-0.41*** ± 0.29	**2.92*** ± 1.72	**8.86*** ± 3.79
	H	**5.45*** ± 3.96	**13.70*** ± 42.49	**101.49** ± 0.52	**17.88*** ± 3.96	**85.47*** ± 12.08	**16.27*** ± 3.00	**21.58** ± 3.82	**0.23** ± 0.13	**184.84*** ± 85.63	**17.66*** ± 5.06	**0.14*** ± 0.07	**5.71*** ± 1.61	**15.91*** ± 5.10
Maturity	L	**8.42*** ± 5.02	**57.66*** ± 57.02	**101.59*** ± 0.45	**22.93*** ± 2.61	**88.13*** ± 10.09	**19.26*** ± 2.36	**25.79*** ± 2.20	**0.19*** ± 0.09	**186.15*** ± 91.92	**24.08*** ± 4.55	**-0.42*** ± 0.30	**1.96*** ±1.32	**24.08*** ± 4.55
	H	**7.01*** ± 4.25	**28.67*** ± 37.21	**101.68*** ± 0.44	**22.21*** ± 2.51	**88.35*** ± 10.10	**18.69*** ± 2.42	**26.45*** ± 2.44	**0.21*** ± 0.11	**167.93*** ± 98.22	**22.69*** ± 4.81	**0.14*** ± 0.08	**4.54*** ±1.70	**22.69*** ± 4.81
Senescence	L	**4.65*** ± 3.74	**67.71*** ± 77.07	**101.87*** ± 0.62	**15.19*** ± 5.25	**84.92*** ± 12.61	**14.64*** ± 4.07	**17.64*** ± 3.84	**0.23*** ± 0.12	**182.81** ± 110.44	**14.93*** ± 6.25	**-0.43*** ± 0.29	**3.11*** ±1.57	**10.66*** ± 3.78
	H	**4.04*** ± 3.55	**38.21*** ± 57.43	**102.10*** ± 0.57	**17.05*** ± 3.83	**87.09*** ± 10.69	**16.03*** ± 3.19	**19.50*** ± 3.08	**0.26*** ± 0.14	**192.32** ± 123.58	**16.71*** ± 4.88	**0.19*** ± 0.13	**4.97*** ±1.67	**14.17*** ± 5.41
Dormancy	L	**1.73** ± 2.03	**19.82** ± 45.74	**102.13** ± 0.89	**6.01*** ± 6.12	**73.86*** ± 18.05	**8.38*** ± 4.65	**7.96*** ± 3.81	**0.29*** ± 0.16	**192.64*** ± 111.87	**6.81*** ± 3.95	**-0.46*** ± 0.28	**5.46*** ±2.40	**8.18*** ± 3.54
	H	**1.91** ± 2.57	**19.42** ± 49.69	**102.04** ± 0.97	**7.09*** ± 5.01	**81.23*** ± 15.20	**9.78*** ± 4.01	**9.93*** ± 3.38	**0.26*** ± 0.16	**158.15*** ± 123.31	**8.32*** ± 3.61	**0.12*** ± 0.08	**7.75*** ±2.05	**13.06*** ± 4.12

L: Low water table level; H: High water table level.
*Significant differences ($p < 0.05$).

(Table 3).

For daytime and nighttime, across phenological phases, WTL showed significant differences between low and high ($p < 0.05$). L-WTL was relatively constant across diel cycles and phenological phases (about -0.4 m), while H-WTL was more variable. Water dissolved oxygen and water salinity increased when WTL increased ($p < 0.05$). PAR, TA, TS, TW and fH2O showed an increase throughout the growing season and phenological phases, some of them (e.g., PAR, TA, fH2O) with significant differences between WTL. The mean values of PA, RH and USTAR were similar across phenological phases; however, some of them (e.g., PA, RH) had significant differences among L-WTL and H-WTL. WD also had changes across phenological phases; almost all of them with significant differences between L-WTL and H-WTL (Tables 2 and 3).

3.3. Biophysical Drivers and Functional Relationships

Different biophysical drivers influenced daytime NEE and daytime CH_4 exchange (Fig. 4a, b). Overall, the CCA was able to explain >44% of daytime NEE variability (Fig. 4a) and <45% of daytime CH_4 exchange (Fig. 4b). Daytime NEE showed a combined positive relationship across phenological phases with PAR, TA and USTAR, with correlations >0.93, >0.45 and >0.42, respectively. Daytime NEE showed a constant negative correlation with RH >-0.42 during phenological phases (Fig. 4a). We found that daytime CH_4 exchange had a positive relationship with TW and fH2O >0.53 and 0.60, respectively; but a negative relationship with WTL, DO and PA >-0.42, >-0.55 and >-0.49, respectively. During Senescence, 45% of daytime CH_4 exchange was explained by the combination of biophysical drivers (Fig. 4b). Similar biophysical drivers related with nighttime NEE and nighttime CH_4 exchange (Fig. 4c, d). During nighttime, both fluxes showed a positive relationship with TW and fH2O >0.50 and >0.52, respectively; but a negative relationship with DO and PA > -0.47. Nighttime CH_4 exchange showed a negative relationship with WTL > -0.45, but nighttime NEE did not show a relationship with WTL.

From the CCA results, we identified key biophysical drivers and we tested independent functional relationships with NEE and CH_4 exchange. We found that 57% to 67% of PAR variability explains daytime NEE when vegetation is active (Table 4). We did not find a single driver that (by itself) could significantly explain daytime or nighttime CH_4 exchange nor nighttime NEE (Table 4). Consequently, these results support the use of the CCA as this analysis identifies how the multivariate space of the independent variables influence NEE and CH_4 exchange.

3.4. NEE and CH_4 exchange Annual Budgets, Global Warming Potential and Sustained-Flux Global Warming Potential

This salt marsh ecosystem was a net source of CO_2 and CH_4 to the atmosphere, with an average annual emission of 138 ±108 g C-CO_2 m^2 and 11.1 ±3.6 g C-CH_4 m^2 (Table 5). We found a constant CO_2 uptake across Maturity with an annual average of -61 ±17 g C-CO_2 m^2, and consistent CO_2 emissions during Senescence and Dormancy, with annual average values of 50 ±25 g C-CO_2 m^2 and 182 ±59 g C-CO_2 m^2, respectively. This ecosystem was also a net source of CH_4 across all phenological phases, with higher emissions across Maturity and Senescence, with an annual average of 3.7 ±1.8 g C-CH_4 m^2 and 4.2 ±4.3 g C-CH_4 m^2, respectively (Table 5).

We found higher intra-annual variability for NEE than for CH_4 exchange (Table 5). NEE had a strong seasonality and large variability among years; for 2016 this ecosystem was almost a neutral CO_2 sink but for the other years there were emissions for about 200 g C-CO_2 m^2. Ecosystem scale CH_4 emissions increased throughout the study period

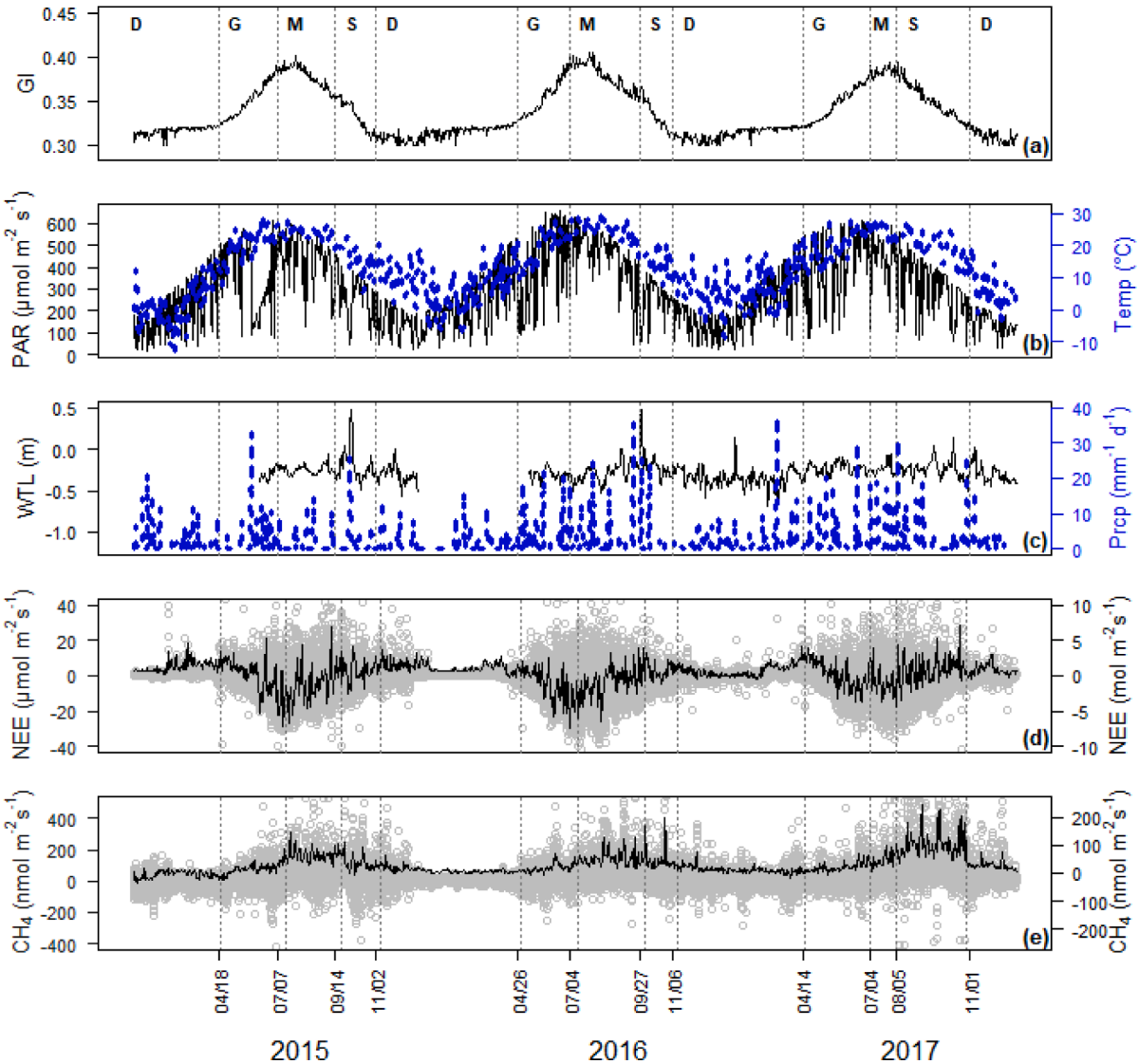

Fig. 1. Phenological phases, ancillary measurements, NEE and CH_4 exchange in the temperate tidal salt marsh from January 2015 to December 2017. (a) Mean daily greenness index (GI) derived from RGB photos from PhenoCam data. GI was used to identify phenological phases in the salt marsh; letters represent those phases (i.e., G:Greenup, M:Maturity; S:Senesncence and D:Dormancy); (b) Mean daily photosynthetically active radiation (PAR; in black) and mean daily air temperature (Temp, in blue); (c) Mean daily water table level (WTL, in black) and daily precipitation (Prcp; in blue); (d) Gap filled NEE, 30 min fluxes are in grey and daily sums are in black line, and (e) Gap filled CH_4 exchange, 30 min fluxes are in grey and daily sums are in black line.

with maximum emissions of 15.2 g C-CH_4 m^2 during 2017 (Table 5).

We found similar results between the GWP and SGWP for NEE and CH_4 exchange for the 20- and 100-year scenarios (Table 6). For both warming potentials CH_4 exchange was higher than NEE for the 20- and 100- year scenarios. NEE warming potential was highest during Dormancy followed by Senescence, Maturity and finally Greenup. CH_4 exchange warming potentials were highest during Senescence and Maturity and were followed by Dormancy and Greenup for both year scenarios (Table 6). Total GWP and SGWP for the 20-year scenarios were positive and higher across all phenological phases than GWP and SGWP for the 100-year scenarios (Table 6).

4. Discussion

Incorporating plant phenology is important to explain the temporal variation of ecosystem-scale NEE and CH_4 exchange in temperate tidal salt marshes dominated by grasses. Our results partially support our first hypothesis, as this ecosystem was a net sink of CO_2 during Maturity and a CO_2 source during Senescence and Dormancy. Contrary to our expectations, the lower but constant CO_2 emissions during Dormancy (i.e., 168 ±3 days and ~45% of an annual cycle) overshadowed the CO_2 uptake during the growing season and contributed for more than 72% of the annual CO_2 emissions by this ecosystem (Table 5). This finding is consistent with spare studies of soil CO_2 fluxes in salt marshes during wintertime (Diefenderfer et al., 2018; Duarte et al., 2014).

We found that low CH_4 emissions were consistent across all phenological phases but were 50% higher across Maturity and Senescence (Table 5). These results highlight the potential role of salt marsh vegetation to transport CH_4 from soils to the atmosphere associated with higher methane production in soils during these phenological phases as a consequence of anaerobic decomposition of available organic matter (Seyfferth et al., 2020). Despite salt marshes being highly productive ecosystems, it is critical to evaluate land-atmosphere CO_2 and CH_4 exchange throughout the complete year to fully evaluate their net carbon sequestration potential.

Our second hypothesis was not supported because we found an increase for ecosystem-scale CO_2 uptake under high water table level (H-WTL) and an increase of daytime and nighttime ecosystem-scale CH_4

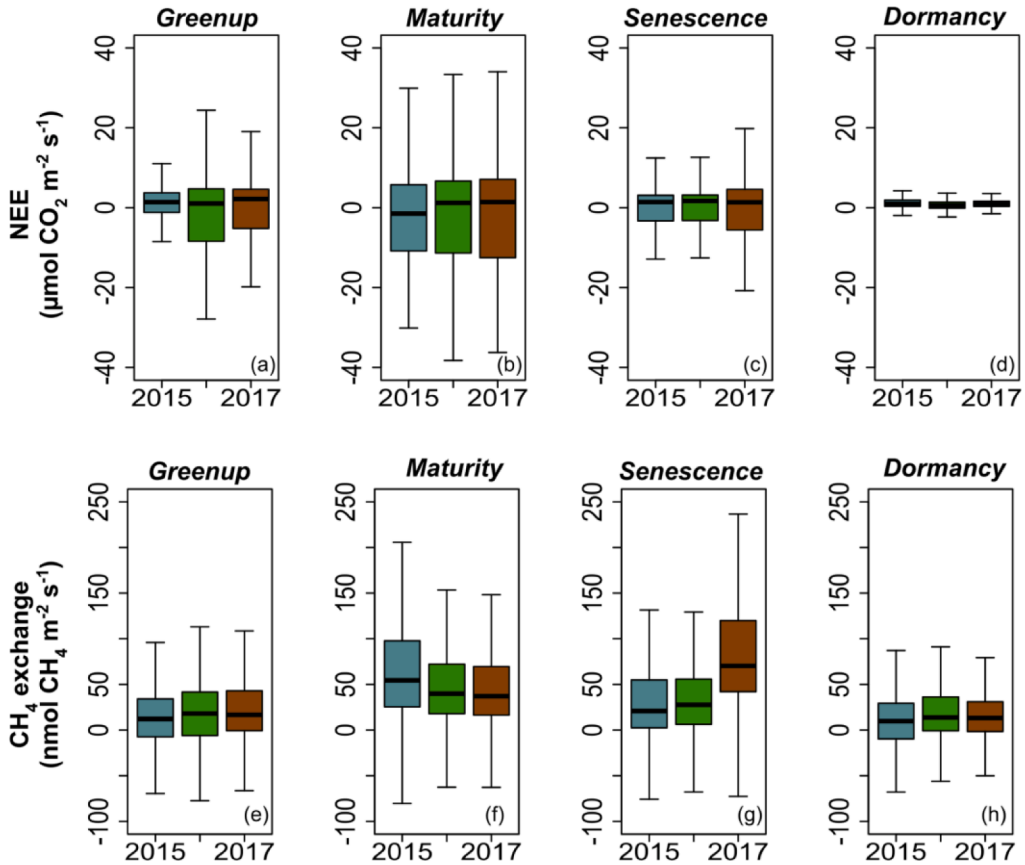

Fig. 2. NEE and CH_4 exchange across phenological phases. NEE showed significant differences among all phenological phases ($p < 0.05$; a-d). CH_4 exchange had significant differences among all phases except Greenup and Dormancy (e-h).

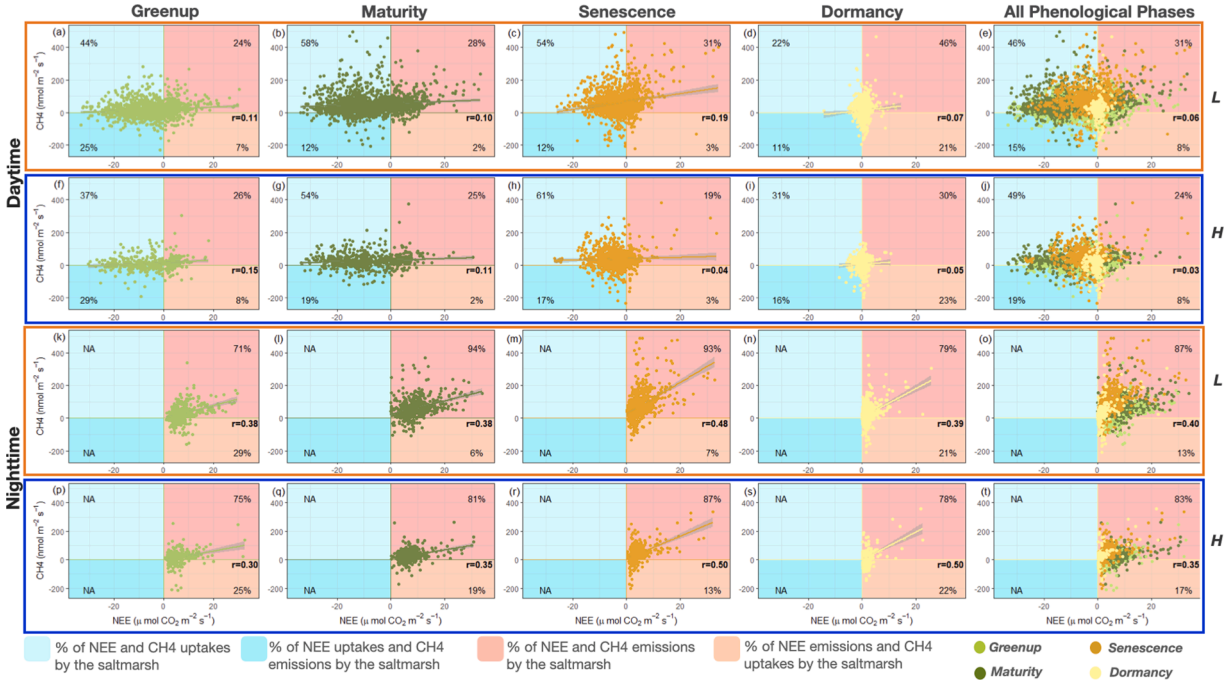

Fig. 3. NEE and CH_4 exchange relationships across phenological phases, daytime/nighttime and WTL. Letters on the right side represent water table levels (L: Low and H: High). Daytime relationships at L-WTL (a-e) and at H-WTL (e-j). Nighttime relationships at L-WTL (k-o) and at H-WTL (p-t). Sub-panels represent the percentage of positive fluxes (i.e., emissions to the atmosphere) and negative fluxes (i.e., uptakes). *r* coefficient represents the linear relationship between NEE and CH_4 exchange.

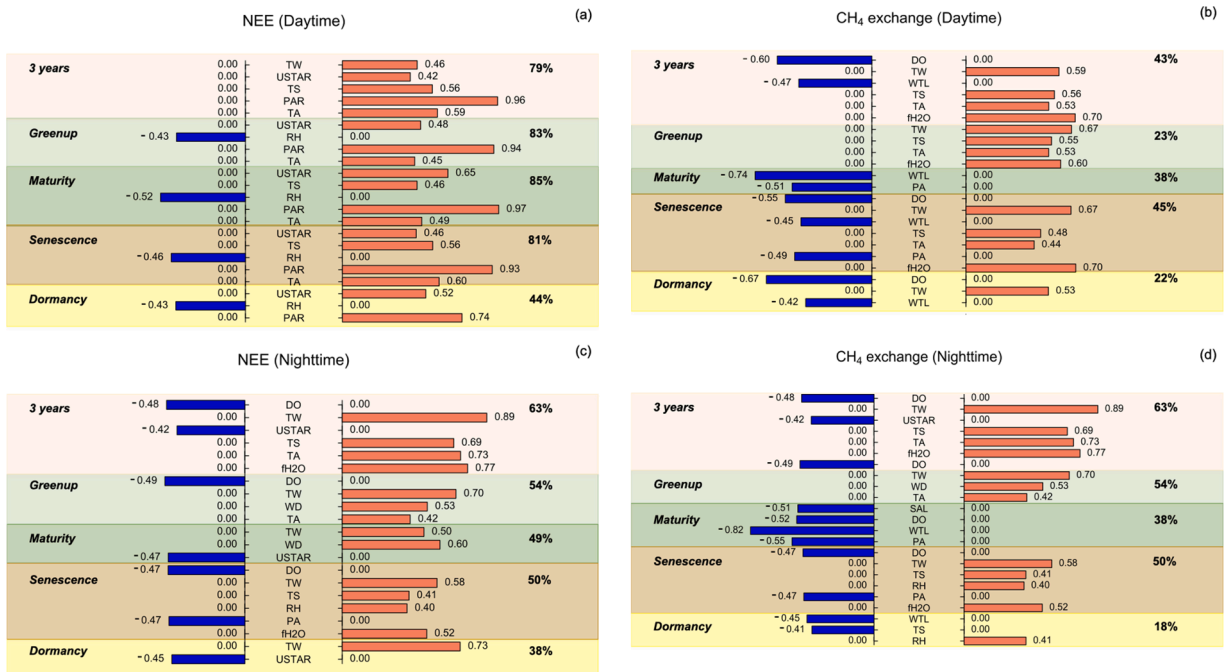

Fig. 4. Biophysical drivers of NEE and CH_4 exchange during daytime (a, b) and nighttime (c, d). Biophysical drivers are at the middle of every panel and their relationship with NEE or CH_4 exchange are represented by the horizontal bars aside of every driver. Values in front of every bar can be interpreted as *r* coefficients for correlations. Orange bars represent positive relationships with the flux and blue bars negative relationships with the flux. Percentage on the right side of every panel represents the explained variance of NEE and CH_4 exchange by phenological phase. Abbreviations of biophysical drivers are: PA (Atmospheric pressure); RH (Relative Humidity); TA (Air Temperature); PAR (Incoming Photosynthetic Active Radiation); TS (Soil Temperature); WTL (Water Table Level); USTAR (Friction Velocity u.); WD (Wind Direction); Water Temperature (TW); DO (Dissolve Oxygen in Water); SAL (Salinity in Water); fH2O (H_2O exchange).

Table 4
Functional relationships of NEE and CH_4 exchange across daytime, nighttime and phenological phases considering single biophysical drivers identified from the CCA analyses (Fig. 4 a- d).

Daytime/Nighttime	Phenology Phase	Biophysical driver	Flux	r^2	p value	y-intercept	Slope [CI > 95%]	Regression model
Daytime	Greenup	PAR	NEE	**0.601**	< 2.2e-16	3.613***	-0.012*** [-0.011]	NEE= 3.613 + (-0.012) PAR
	Maturity	PAR	NEE	**0.670**	< 2.2e-16	4.594***	-0.016*** [-0.015]	NEE= 4.594 + (-0.015) PAR
	Senescence	PAR	NEE	**0.568**	< 2.2e-16	3.086***	-0.011*** [-0.010]	NEE= 3.086 + (-0.010) PAR
	Dormancy	PAR	NEE	0.103	< 2.2e-16	0.894**	-0.002*** [-0.001]	NEE= 0.894 + (-0.002) PAR
	Greenup	TW	CH_4	0.020	2.01e-09	-22.022***	1.73*** [2.29]	CH_4= -22.022 + 1.73 TW
	Maturity	WTL	CH_4	0.079	< 2.2e-16	30.412***	-50.593*** [-43.540]	CH_4= 30.412 + (-50.593) WTL
	Senescence	fH2O	CH_4	0.101	< 2.2e-16	-11.019***	3.954*** [4.433]	CH_4= -11.019 + (3.954) fH2O
	Dormancy	DO	CH_4	0.019	5.378e-10	25.797***	-2.254*** [-1.550]	CH_4= 25.797 + (-2.254) DO
Nighttime	Greenup	TW	NEE	0.144	< 2.2e-16	-2.99***	0.445*** [0.515]	NEE= -2.99 + (0.445) TW
	Maturity	WD	NEE	0.100	< 2.2e-16	4.99***	0.016*** [0.018]	NEE= 4.99 + (0.016) WD
	Senescence	TW	NEE	0.066	< 2.2e-16	-0.251***	0.256*** [0.305]	NEE= -0.251 + (0.256) TW
	Dormancy	TW	NEE	0.070	< 2.2e-16	0.498***	0.151*** [0.180]	NEE= 0.498 + (0.151) TW
	Greenup	TW	CH_4	0.010	0.001134	-6.60	1.301** [2.082]	CH_4= -6.60 + (1.301) TW
	Maturity	WTL	CH_4	0.100	< 2.2e-16	36.980***	-45.362*** [-37.730]	CH_4= 36.980 + (-45.362) WTL
	Senescence	TW	CH_4	0.0634	< 2.2e-16	-32.845***	4.930*** [5.88]	CH_4= -32.845 + (-4.93) TW
	Dormancy	WTL	CH_4	0.003	0.02337	17.082	-8.175 [-1.110]	CH_4= 17.082 + (-8.175) WTL

** $p < 0.01$; *** $p < 0.001$.

Table 5
NEE and CH_4 exchange carbon budgets for each phenological phase and for each year.

Phenological Phase/Year	NEE (g C-CO_2 m^2)				CH_4 Exchange (g C-CH_4 m^2)			
	2015	2016	2017	All years (mean)	2015	2016	2017	All years (mean)
Greenup	-14	-99	15	-33	1.4	1.4	1.8	1.6
Maturity	-74	-68	-42	-61	4.7	4.8	1.7	3.7
Senescence	39	33	79	50	1.8	1.6	9.2	4.2
Dormancy	250	147	148	182	0.6	1.9	2.5	1.7
Total (g C m-2)	*201*	*13*	*200*	*138*	*8.5*	*9.7*	*15.2*	*11.1*

Table 6
Mean Global Warming Potential and Mean Sustained-Flux Global Warming Potential of NEE and CH_4 exchange from this salt marsh to the atmosphere for a 20- and 100-year scenarios.

Phenology Phase/Year	Mean NEE ($CO_{2\text{-eq}}$ g m^{-2}) 20 and 100 year scenarios		Mean CH_4 exchange ($CO_{2\text{-eq}}$ g m^{-2}) 20-year scenarios		Mean CH_4 exchange ($CO_{2\text{-eq}}$ g m^{-2}) 100-year scenarios		Total mean ($CO_{2\text{-eq}}$ g m^{-2})			
	GWP	SGWP	GWP	SGWP	GWP	SWGP	20-year GWP	100-year GWP	20-year SGWP	100-year SGWP
Greenup	-121	-121	181	200	67	94	60	-54	79	-27
Maturity	-225	-225	431	475	158	223	206	-67	250	-2
Senescence	184	184	487	538	179	252	671	363	722	436
Dormancy	666	666	197	217	73	102	863	739	883	768
Total	504	504	1,296	1,430	477	671	1,800	981	1,934	1,175

emissions with low water table level (L-WTL). These results contrast with previous findings about the decrease for CO_2 uptake with H-WTL (Forbrich and Giblin, 2015; Kathilankal et al., 2008), and increase for CH_4 emissions with H-WTL (Holm et al., 2016; Krauss et al., 2016). WTL plays an important role for regulating ecosystem-scale CO_2 and CH_4 exchange in salt marshes, but its influence seems to be site-specific and influenced by the spatial heterogeneity of these ecosystems (i.e., local geomorphology, soil properties and species composition; Knox et al., 2019; Negandhi et al., 2019; Ward et al., 2020;).

Our third hypothesis was partially supported by our results because PAR was the main driver of daytime NEE when vegetation was active, but not during Dormancy, when CO_2 emissions overshadowed CO_2 uptake as most vegetation is inactive. We did not find a single driver that substantially explained nighttime NEE nor daytime and nighttime CH_4 exchange, thus, emphasizing the challenge for modelling both fluxes in salt marsh ecosystems (Al-haj and Fulweiler, 2020; Li et al., 2018). The implications of these findings are: a) the use of PAR to model daytime NEE (without including other confounding effects; e.g., WTL) may overestimate net annual CO_2 uptake. This may be more relevant during Dormancy when factors controlling the ecosystem respiration could have a higher influence than PAR (Bonneville et al., 2008; Diefenderfer et al., 2018); and b) CH_4 emissions cannot be neglected (neither for site-measurements nor for modeling) because these low albeit constant emissions contribute to overall carbon losses from this ecosystem (Al-haj and Fulweiler, 2020); and c) changes in plant phenological phases should be considered to explain CO_2 and CH_4 exchange in temperate salt marsh ecosystems and measurements should extend beyond the growing season.

4.1. Influence of plant phenology on NEE and CH_4 exchange

Plant phenological phases are relevant to explain the exchange of carbon in this ecosystem. It is known that during Maturity, there is an increase in aboveground carbon allocation and shoot height (Crosby et al., 2015), and likely these structures favor higher net daily CO_2 uptake. These findings are consistent with Artigas et al. (2015), Forbrich and Giblin (2015) and Schäfer et al. (2014) that found higher CO_2 uptake in salt marsh ecosystems during the peak of the growing season across the Mid-Atlantic region of USA, as well as other regions of the world (e.g., South America: Tonti et al., 2018; China: Chu et al., 2018).

During Maturity it is also expected that marsh vegetation had fully developed aerenchyma tissue to oxygenate the root system (Maricle and Lee, 2002); consequently, these structures favor the transport of CH_4 and CO_2 from soils to the atmosphere by molecular diffusion or convective pressurization mechanisms (Kludze and Delaune, 1994; Joabson et al., 1999; Waldo et al., 2019). These abiotic processes could account between ~50 to >90% of the total CH_4 exchange in salt marsh mesocosms (Kludze and Delaune, 1994), and has been documented for other temperate saltmarshes dominated by aerenchymatous vegetation (Ford et al., 2012).

Onset of senescence was very variable as well as the amount of NEE and CH_4 exchange during this phenological phase. During this phase, there is likely a shift on plant carbon allocation from aboveground to belowground, increasing their root surface area and the production of root exudates (Crosby et al., 2015; O'Connell et al., 2020); consequently, resulting in an increase of CO_2 emissions by the root system respiration, decrease of photosynthesis, and an increase of microbial activity to decompose root exudates (Girkin et al., 2018; Waldo et al., 2019). For our study site, it is likely that canopy defoliation during Senescence contributes to substrates for methanogenesis in the soils (i.e., methylotrophic methanogenesis; Seyfferth et al., 2020). Our results are consistent with findings in salt marshes that shifted from being a CO_2 sink during warmer months to a CO_2 source after the onset of Senescence (Artigas et al., 2015; Forbrich et al., 2018). The increase of CH_4 emissions during Senescence is also consistent with findings in brackish and freshwater marshes in the Gulf of Mexico (Krauss et al., 2016) and from mangrove forests in South China (Liu et al., 2020).

Dormancy was the longest (~168 days) and less variable phenological phase. It showed low but constant CO_2 and CH_4 emissions; likely derived from emissions from soils and water from creeks as a consequence of soil respiration and CH_4 ebullition (Diefenderfer et al., 2018; Seyfferth et al., 2020; Trifunovic et al., 2020). We highlight that CH_4 emitted in our study site represents a small portion of the CH_4 stored in soils (i.e., at least ~ 892 μM; Seyfferth et al., 2020); thus, a relevant proportion of that CH_4 may follow different pathways before being emitted to the atmosphere (e.g., CH_4 oxidation, lateral transport; Trifunovic et al., 2020). We advocate for year round measurements of CO_2 and CH_4 to fully account for emissions during wintertime that could be relevant contributors for the annual carbon budget in temperate tidal salt marshes (Al-haj and Fulweiler, 2020; Diefenderfer et al., 2018).

4.2. Influence of WTL and other biophysical drivers during daytime and nighttime on NEE and CH_4 exchange

Water table level is a key driver controlling the biogeochemical cycles that influence NEE and CH_4 exchange in coastal wetlands on a diel cycle. We found that WTL had a significant influence on NEE and CH_4 exchange (Table 2 and 3); however, when WTL was combined with other biophysical drivers it was only significant for CH_4 exchange. These results add to the growing evidence of confounding effects and their challenge for modelling biogenic fluxes in these ecosystems (Knox et al., 2019; Knox et al., 2018; Li et al., 2018; Trifunovic et al., 2020).

We found an increase of CO_2 uptake with H-WTL and an increase of nighttime CO_2 emissions with L-WTL. The increase of CO_2 uptake within H-WTL is consistent with some findings in salt marshes (Artigas et al., 2015, Guo et al., 2009, Knox et al., 2018 and Schäfer et al., 2014), but contrast with other observations that attributed a decrease of CO_2 uptake because of total or partial flooding of the vegetation (Forbrich and Giblin, 2015, Kathilankal et al., 2008 and Moffett et al., 2010). The salt marsh grasses in our study site are not fully submerged during H-WTL in the semidiurnal tidal cycle. In addition, an increase of CO_2 uptake could be a consequence of an increase of DO in the water during H-WTL (Table 2) that could enhance plant photosynthesis as in other studies (Maricle and Lee, 2007). Another possibility could be the lateral loss of dissolved CO_2 in the water during H-WTL, that can be transported out of the EC footprint and not measured when it is emitted to the atmosphere (Schäfer et al., 2019; Trifunovic et al., 2020). As a seen in our study, nighttime CO_2 emissions increased with L-WTL (Table 3), possible as a consequence of an increase of diffusivity rates of CO_2 in the salt marsh soils, mainly in areas close to creeks, that are constantly exposed to WTL oscilations (Seyfferth et al., 2020).

Ecosystem-scale CH_4 emissions increase during L-WTL. These findings are consistent with Li et al. (2018), but contrast with Holm et al., (2016) that found an increase of CH_4 exchange when WTL increased on freshwater and brackish marshes in Louisiana, attributing this result to an increase of anaerobic conditions and a higher CH_4 production. We attribute our findings to an emergent property of this salt marsh ecosystem, where the exposition of soils during L-WTL increasing the soil CH_4 diffusivity, and likely have lower salinity (Table 2 and 3) which may increase methanogenesis as seen in other studies (Capooci et al., 2019; Poffenbarger et al., 2011).

There are contrasting biophysical drivers for daytime and nighttime NEE and CH_4 exchange. Consistent with other studies, light availability (PAR) was the most significant driver of daytime NEE (Knox et al. 2018, Schäfer et al. 2014, Zhong et al 2016). We also found a positive relationship between NEE and USTAR, possibly because USTAR influences the diffusion rate of CO_2 in the atmosphere and consequently its vertical exchange (Chu, 2014). For CH_4 exchange, we found that a combination of biophysical drivers is needed to explain its temporal variability. A positive relationship of TW and fH2O, and a negative relationship of WTL, DO and PA explained daytime CH_4 exchange. TW had a mayor influence on CH_4 exchange than soil or air temperature, possibly because it may have a mayor influence on the biogeochemical processes that control CH_4 production and its emission from the salt marsh soils and water surface layers (i.e., methanogenesis and ebullition; Kim et al., 1999; Seyfferth et al., 2020; Trifunovic et al., 2020; Rey-Sanchez et al., 2018). A positive relationship of fH2O with daytime CH_4 exchange could be a confounded factor, because fH2O and CH_4 exchange may happen at the same time when both gases are moved through the vegetation. Negative relationship of DO with daytime CH_4 exchange could be because DO may increase aerobic conditions in the salt marsh soils that reduce the CH_4 production (Flury et al., 2010). Furthermore, a drop of PA may facilitate the ebullition of methane from the water surface layer and its diffusion in the salt marsh soils by the reduction of atmospheric pressure on them (Oertel et al., 2016; Rey-Sanchez et al., 2018; Tokida et al., 2007). Our findings showed the need to better identify the combined influence of different biophysical drivers on NEE and CH_4 exchange in salt marsh ecosystems across phenological phases, daytime and nighttime, to better represent those fluxes in ecosystem-process models.

Our results showed that NEE had higher interannual variability than CH_4 exchange, where the ecosystem was almost carbon neutral during 2016 and a net source for the other years. Interannual variability could be influenced by PAR, as levels in 2016 were 10% higher than 2015 and 5% higher than 2017. Higher PAR may have resulted in higher gross primary production (GPP) during 2016 (about 10% higher GPP than during other years (results not showed)). Other studies have found an increase in GPP with PAR for salt marsh ecosystems (Knox et al., 2018; Zhong et al., 2016) and this relationship is consistent for regional models of GPP for coastal wetlands (Feagin et al., 2020).

A complementary explanation for high interannual variability in NEE could be related to changes in ecosystem respiration (Reco). We postulate that Reco may have been 17% and 13% higher than GPP for 2015 and 2017, but similar to GPP during 2016 (data not shown). We clarify that the Greenup phenological phase during 2016 was mainly responsible of CO_2 uptake during that year (Table 5), but it was shorter compared to 2015 and 2017 (i.e., 8 days shorter that Greenup during 2015 and 17 days shorter than Greenup phase during 2018).

NEE and CH_4 exchange from salt mash ecosystems are poorly represented in ecosystem process models and earth system models. In general, the drivers commonly used to model carbon exchange: a) rely on generalizations form terrestrial ecosystem processes, that may not fully explain NEE and CH_4 exchange variability in salt marshes (Frolking et al., 1998; Knox et al., 2019; Poulter et al., 2014); b) lack representation and accountability of lateral transport of CO_2 and CH_4 *in*-and-*out* of the ecosystem impact the accounting of carbon that is fixed, stored and lost (Duman and Schäfer, 2018; Trifunovic et al., 2020; Van de Broek et al., 2018); and c) are an oversimplification of the spatial and temporal heterogeneity of coastal wetlands (Ward et al., 2020). In addition, CH_4 emissions from salt marshes may be overlooked or even neglected by following the assumption that constant salinity and sulfate inputs may reduce or inhibit methanogenesis, but alternative methanogenesis pathways in sulfate-rich sediments (e.g., methylotrophic methanogenesis) should be revisited to improve ecosystem-process models (Seyfferth et al., 2020).

4.3. Carbon budgets in the salt marsh and warming potentials

"Blue Carbon" refers to organic carbon that is captured and stored by coastal ecosystems (i.e., autochthonous and allochthonous carbon; (Van de Broek et al., 2018)), including vegetated coastal ecosystems such as salt marshes (McLeod et al., 2011). However there are knowledge gaps in the blue carbon paradigm, where ecosystem processes sometimes offset the capacity of these ecosystems to fix and store carbon (Macreadie et al., 2019; Rosentreter et al., 2018; Liu et al., 2020).

This temperate tidal salt marsh was a net source of carbon to the atmosphere with 92% higher carbon emissions from CO_2 than from CH_4. Our average values of carbon emitted as CO_2 (Table 5) were similar or more than two times higher than values reported for other herbaceous coastal wetlands at equal and higher latitudes (Lu et al., 2017). Our study site emitted ~2 times less carbon as CO_2 than other non-impacted salt marshes, and ~10 times less than urban restored salt marshes (Schäfer et al., 2019). Our values of carbon emitted as CH_4 were between the range of CH_4 emission reported for salt marshes (Poffenbarger et al., 2011; Knox et al., 2019), and similar to values reported for brackish marshes in the Gulf of Mexico (Krauss et al., 2016).

Substantial but constant lower CH_4 emissions across the study period had a 64% higher SGWP than CO_2 in a 20-year scenario, and 25% higher SGWP than CO_2 in a 100-year scenario. We highlight that these calculations were not significantly different than using the global warming potential (GWP) as done in previous studies (Capooci et al., 2019; Petrakis et al., 2017). SGWP is a relative new metric that could be used as an alternative to represent sustained contributions or cooling effects from

natural ecosystems (Neubauer and Megonigal, 2019); however, more studies are needed to compare estimates of GWP and SGWP to identify discrepancies in coastal wetlands. We postulate that the local geomorphology heterogeneity and its influence on hydrology and quality of soil organic carbon (Seyfferth et al., 2020), as well as hotspots of CO_2 and CH_4 emissions from surface water (Trifunovic et al., 2020), influence this salt marsh to be a net carbon source. More research is needed at different temporal and spatial scales across the different components of salt marsh ecosystems (i.e., vegetation types, water and soils) to properly attribute how local heterogeneity and phenology phases could influence annual carbon budgets.

Our plant-phenological phase approach and its influence on the ecosystem-scale NEE and CH_4 exchange could be considered for future studies in wetlands dominated by grasses. This approach could be useful to better understand the role of wintertime on the exchange of carbon in temperate marshes, and reduce the bias information on the limited literature that usually focus to report results for the growing season (Forbrich and Giblin, 2015; Kathilankal et al., 2008). In addition, it may help to better understand the effects of human activities on marshes (i.e., managed areas for grazing) and their potential implications for carbon dynamics (Davidson et al., 2017; Harvey et al., 2019). Finally, our results are useful to monitor and understand the carbon cycle in temperate coastal wetlands (Ward et al., 2020), to reduce the uncertainty of the carbon exchanged within the atmosphere for synthesis studies (Holmquist et al., 2018; Knox et al., 2019; Lu et al., 2017), and to improve models of blue carbon at the national scale (Byrd et al., 2018; Feagin et al., 2020).

5. Conclusions

Our results show that plant phenological phases are relevant to explain the temporal variability of NEE and CH_4 exchange in this tidal salt marsh. Daytime NEE was partially influenced by the availability of light during the growing phases, while daytime and nighttime CH_4 exchange was influenced by the combination of different biophysical drivers, including WTL. Our findings explain less variability for CH_4 exchange than NEE, highlighting the difficulties to model CH_4 exchange in these ecosystems. This tidal salt marsh was a net source of carbon to the atmosphere, with higher global warming potentials from CH_4 emissions than CO_2 emissions. Our findings challenge the general expectation that blue carbon ecosystems should be net sinks of carbon, and highlight the need to perform flux measurements throughout the whole year to properly assess the net land-atmosphere exchange of CO_2 and CH_4 in temperate tidal salt marshes.

Declaration of Competing Interest

The authors declare that they have no known competing financial interests or personal relationships that could have appeared to influence the work reported in this paper.

Acknowledgements

AVL acknowledges support from the National Council for Science and Technology (CONACYT, Mexico; fellowship #240634/440832) and a Delaware Environmental Graduate Fellowship (DENIN). RV acknowledges support from the National Science Foundation (#1652594). We thank the onsite support from the Delaware National Estuarine Research Reserve (DNERR), and Mario Guevara for advice to develop the ANNvDL gap-filling code.

Authors acknowledge the land on which they realized this study as the traditional home of the Lenni-Lenape tribal nation (Delaware nation). Authors acknowledge the feedback of two anonymous reviewers.

Supplementary materials

Supplementary material associated with this article can be found, in the online version, at doi:10.1016/j.agrformet.2020.108309.

References

Al-haj, A.N., Fulweiler, R.W., 2020. RESEARCH REVIEW A synthesis of methane emissions from shallow vegetated coastal ecosystems 2017, 2988–3005. doi:10.1111/gcb.15046.

Artigas, F., Shin, J.Y., Hobble, C., Marti-Donati, A., Schäfer, K.V.R., Pechmann, I., 2015. Long term carbon storage potential and CO2 sink strength of a restored salt marsh in New Jersey. Agric. For. Meteorol. 200, 313–321. https://doi.org/10.1016/j.agrformet.2014.09.012.

Bauer, J.E, Cai, W.-J., Raymond, P.A., Bianchi, T.S., Hopkinson, C.S., Regnier, P.A.G., 2013. The changing carbon cycle of the coastal ocean. Nature 504, 61–70. https://doi.org/10.1038/nature12857.

Bonneville, M., Strachan, I.B., Humphreys, E.R., Roulet, N.T., 2008. Net ecosystem CO 2 exchange in a temperate cattail marsh in relation to biophysical properties 148, 69–81. doi:10.1016/j.agrformet.2007.09.004.

Bridgham, S.D., Megonigal, J.P., Keller, J.K., Bliss, N.B., Trettin, C., 2006. The carbon balance of North American wetlands. Wetlands 26, 889–916. https://doi.org/10.1672/0277-5212(2006)26[889:TCBONA]2.0.CO;2.

Byrd, K.B., Ballanti, L., Thomas, N., Nguyen, D., Holmquist, J.R., Simard, M., 2018. ISPRS Journal of Photogrammetry and Remote Sensing A remote sensing-based model of tidal marsh aboveground carbon stocks for the conterminous United States. ISPRS J. Photogramm. Remote Sens. 139, 255–271. https://doi.org/10.1016/j.isprsjprs.2018.03.019.

Capooci, M., Barba, J., Seyfferth, A.L., Vargas, R., 2019. Science of the Total Environment Experimental in fl uence of storm-surge salinity on soil greenhouse gas emissions from a tidal salt marsh. Sci. Total Environ. 686, 1164–1172. https://doi.org/10.1016/j.scitotenv.2019.06.032.

CEC, 2015. Marsh Carbon Storage in the National Estuarine Research Reserves, USA: A Comparison of Methodologies and Coastal Regions, 67. Commission for Environmental Cooperation, Montreal, Canada.

Chanton, J.P., Arkebauer, T.J., Harden, H.S., Verma, S.B., 2002. Diel variation in lacunal CH 4 and CO 2 concentration and δ 13 C in Phragmites australis. Biogeochemistry 59, 287–301.

Chu, H. et al, 2014. Net ecosystem methane and carbon dioxide exchanges in a Lake Erie coastal marsh and a nearby cropland 722–740. https://doi.org/10.1002/2013JG002520. Received.

Chu, X., Han, G., Xing, Q., Xia, J., Sun, B., Yu, J., Li, D., 2018. Dual effect of precipitation redistribution on net ecosystem CO2 exchange of a coastal wetland in the Yellow River Delta. Agric. For. Meteorol. 249, 286–296. https://doi.org/10.1016/j.agrformet.2017.11.002.

Crosby, S.C., Angermeyer, A., Adler, J.M., Bertness, M.D., Deegan, L.A., Sibinga, N., Leslie, H.M., 2016. Spartina alterniflora Biomass Allocation and Temperature: Implications for Salt Marsh Persistence with Sea-Level Rise. Estuaries and Coasts 1–11. https://doi.org/10.1007/s12237-016-0142-9.

Crosby, S.C., Ivens-Duran, M., Bertness, M.D., Davey, E., Deegan, L.A., Leslie, H.M., 2015. Flowering and biomass allocation in U.S. Atlantic coast Spartina alterniflora. Am. J. Bot. 102, 669–676. https://doi.org/10.3732/ajb.1400534.

Davidson, K.E., Fowler, M.S., Skov, M.W., Doerr, S.H., Beaumont, N., Griffin, J.N., 2017. Livestock grazing alters multiple ecosystem properties and services in salt marshes : a meta-analysis 1395–1405. doi:10.1111/1365-2664.12892.

Diefenderfer, H.L., Gunn, M., Cullinan, V.I., Borde, A.B., Thom, R.M., 2018. High - frequency greenhouse gas flux measurement system detects winter storm surge effects on salt marsh 5961–5971. doi:10.1111/gcb.14430.

Duarte, B., Freitas, J., Valentim, J., Paulo, J., Lino, J., Silva, H., Miguel, J., José, M., Carlos, J., Caçador, I., 2014. Abiotic control modelling of salt marsh sediments respiratory CO 2 fl uxes : application to increasing temperature scenarios. Ecol. Indic. 46, 110–118. https://doi.org/10.1016/j.ecolind.2014.06.018.

Duman, T., Schäfer, K.V.R., 2018. Partitioning net ecosystem carbon exchange of native and invasive plant communities by vegetation cover in an urban tidal wetland in the New Jersey Meadowlands (USA). Ecol. Eng. 114, 16–24. https://doi.org/10.1016/j.ecoleng.2017.08.031.

Feagin, R.A., Forbrich, I., Huff, T.P., Barr, J., Ruiz-Plancarte, J., Fuentes, J.D., Najjar, R., Vargas, R., Vázquez-Lule, A., Windham-Myers, L., Kroeger, K., Ward, E., Moore, G., Leclerc, M.Y., Krauss, K., Stagg, C., Alber, M., Knox, S., Schäfer, K.V., Bianchi, T.S., Hutchings, J., Nahrawi, H., Noormets, A., Mitra, B., Jaimes, A., Hinson, A., Bergamaschi, B., King, J., Miao, G., 2020. Tidal wetland Gross Primary Production across the continental United States, 2000-2019. Global Biogeochemical Cycles 34 (2), e2019GB006349. https://doi.org/10.1029/2019GB006349.

Filippa, G., Cremonese, E., Migliavacca, M., Galvagno, M., Forkel, M., Wingate, L., Tomelleri, E., Morra, U., Richardson, A.D., 2016. Agricultural and Forest Meteorology Phenopix : A R package for image-based vegetation phenology. Agric. For. Meteorol. 220, 141–150. https://doi.org/10.1016/j.agrformet.2016.01.006.

Flury, S., Mcginnis, D.F., Gessner, M.O., 2010. Methane emissions from a freshwater marsh in response to experimentally simulated global warming and nitrogen enrichment 115, 1–9. doi:10.1029/2009JG001079.

Forbrich, Inke, Giblin, Anne, 2015. Marsh-atmosphere CO_2 exchange in a New England salt marsh. Journal of Geophysical Research: Biogeosciences 120 (9), 1825–1838.

Forbrich, I., Giblin, A.E., Hopkinson, C.S., 2018. Constraining Marsh Carbon Budgets Using Long-Term C Burial and Contemporary Atmospheric CO2 Fluxes. J. Geophys. Res. Biogeosciences 123, 867–878. https://doi.org/10.1002/2017JG004336.

Ford, H., Garbutt, A., Jones, L., Jones, D.L., 2012. Estuarine, Coastal and Shelf Science Methane, carbon dioxide and nitrous oxide fl uxes from a temperate salt marsh : Grazing management does not alter Global Warming Potential. Estuar. Coast. Shelf Sci. 113, 182–191. https://doi.org/10.1016/j.ecss.2012.08.002.

Frolking, S.E., Bubier, J.L., Moore, T.R., Ball, T., Bellisario, L.M., Crill, P.M., Lafleur, P. M., Mccaughey, J.H., Roulet, N.T., Suyker, A.E., Verrna, S.B., Waddington, J.M., Whiting, G.J., 1998. Relationship between ecosystem productivity and photosynthetically active radiation for northern peatlands s canopy 12, 115–126.

Gedan, K.B., Silliman, B.R., Bertness, M.D., 2009. Centuries of human-driven change in salt marsh ecosystems. Ann. Rev. Mar. Sci. 1, 117–141. https://doi.org/10.1146/annurev.marine.010908.163930.

Ghosh, S., Mishra, D.R., 2017. Analyzing the Long-Term Phenological Trends of Salt Marsh Ecosystem across Coastal LOUISIANA. doi:10.3390/rs9121340.

Girkin, N.T., Turner, B.L., Ostle, N., Craigon, J., Sjögersten, S., 2018. Root exudate analogues accelerate CO 2 and CH 4 production in tropical peat. Soil Biol. Biochem. 117, 48–55. https://doi.org/10.1016/j.soilbio.2017.11.008.

Gu, L., Post, W.M., Baldocchi, D.D., Black, T.A., Suyker, A.E., Verma, S.B., Vesala, T., Wofsy, S.C., 2009. Characterizing the Seasonal Dynamics of Plant Community Photosynthesis Across a Range of Vegetation Types Characterizing the Seasonal Dynamics of Plant Community Photosynthesis Across a Range of Vegetation Types. doi:10.1007/978-1-4419-0026-5.

Hardoon, D.R., Shawe-taylor, J., 2004. Canonical Correlation Analysis : An Overview with Application to Learning Methods 2664, 2639–2664.

Harvey, R.J., Garbutt, A., Hawkins, S.J., Skov, M.W., 2019. No Detectable Broad-Scale Effect of Livestock Grazing on Soil Blue-Carbon Stock in Salt Marshes 7, 1–12. doi:10.3389/fevo.2019.00151.

González, I., Déjean, S., Martin, P.G.P., Baccini, A., 2008. CCA: An R packege to extend canonical correlation analysis. Journal of Statistical Software 23, 12.

Guo, H., Noormets, A., Zhao, B., Chen, Jiquan, Sun, G., Gu, Y., Li, B., Chen, Jiakuan, 2009. Tidal effects on net ecosystem exchange of carbon in an estuarine wetland. Agric. For. Meteorol. 149, 1820–1828. https://doi.org/10.1016/j.agrformet.2009.06.010.

Hayes, D.R., Vargas, R., Alin, S.R., Conant, R., Hutyra, L.H.T., Jacobson, A.R., Kurz, W. A., 2018. Chapter 2: The North American Carbon Budget. In: Cavallaro, N., Shrestha, G., Birdsey, R., Mayes, M.A., Najjar, R.G., Reed, S.C., Romero-Lankao, Zhu, Z.P. (Eds.), *Second State of the Carbon Cycle Report (SOCCR2): A Sustained Assessment Report*. U.S. Global Change Research Program, Washington, DC, USA, pp. 71–108. https://doi.org/10.7930/SOCCR2.2018.Ch2.

Holm, G.O., Perez, B.C., McWhorter, D.E., Krauss, K.W., Johnson, D.J., Raynie, R.C., Killebrew, C.J., 2016. Ecosystem Level Methane Fluxes from Tidal Freshwater and Brackish Marshes of the Mississippi River Delta: Implications for Coastal Wetland Carbon Projects. Wetlands 36, 401–413. https://doi.org/10.1007/s13157-016-0746-7.

Holmquist, J.R., Windham-myers, L., Bernal, B., Byrd, K.B., Crooks, S., Gonneea, M.E., Herold, N., Knox, S.H., Kroeger, K.D., Mccombs, J., Megonigal, J.P., Lu, M., Morris, J.T., Sutton-grier, A.E., 2018. Uncertainty in United States coastal wetland greenhouse gas inventorying Uncertainty in United States coastal wetland greenhouse gas inventorying.

Jia, Q., Yu, W., Zhou, L., Liang, C., 2017. Atmospheric and surface-condition effects on CO_2 Exchange in the Liaohe Delta Wetland, China. Water 9, 806.

Kathilankal, James C., Mozdzer, T.J., Fuentes, J.D., D'Odorico, P., McGlathery, K.J., Zieman, J.C., 2008. Tidal influences on carbon assimilation by a salt marsh. Environ. Res. Lett. 3 https://doi.org/10.1088/1748-9326/3/4/044010.

Joabson, A., Christensen, T. R., Wallen, B., 1999. Vascular plant controls on methane emissions from northern peatforming wetlands. TREE 10, 385:388.

Kim, J., Hwang, T., Schaaf, C.L., Kljun, N., Munger, J.W., 2018. Agricultural and Forest Meteorology Seasonal variation of source contributions to eddy-covariance CO 2 measurements in a mixed hardwood-conifer forest 254, 71–83. doi:10.1016/j.agrformet.2018.02.004.

Kim, Y., Johnson, M.S., Knox, S.H., Black, T.A., Baldocchi, D., Kim, J., 2020. Gap - filling approaches for eddy covariance methane fluxes : A comparison of three machine learning algorithms and a traditional method with principal component analysis. Glob Chang Biol 26, 1499–1518. https://doi.org/10.1111/gcb.14845.

Kirwan, M.L., Guntenspergen, G.R., Morris, J.T., 2009. Latitudinal trends in Spartina alterniflora productivity and the response of coastal marshes to global change. Glob. Chang. Biol. 15, 1982–1989. https://doi.org/10.1111/j.1365-2486.2008.01834.x.

Kludze, H.K., Delaune, R.D., 1994. Methane Emissions and Growth of Spartina patens in Response to Soil Redox Intensity. Soil Science Society of America Journal 58 (6), 1838–1845.

Knox, Sara H. et al., 2019, 2019. Fluxnet-ch 4 synthesis activity. doi:10.1175/BAMS-D-18-0268.1.

Knox, S.H., Dronova, I., Sturtevant, C., Oikawa, P.Y., Matthes, J.H., Verfaillie, J., Baldocchi, D., 2017. Using digital camera and Landsat imagery with eddy covariance data to model gross primary production in restored wetlands. Agric. For. Meteorol. 237–238, 233–245. https://doi.org/10.1016/j.agrformet.2017.02.020.

Knox, S.H., Windham-Myers, L., Anderson, F., Sturtevant, C., Bergamaschi, B., 2018. Direct and Indirect Effects of Tides on Ecosystem-Scale CO2Exchange in a Brackish Tidal Marsh in Northern California. J. Geophys. Res. Biogeosciences 123, 787–806. https://doi.org/10.1002/2017JG004048.

Krauss, Ken W., Holm, G.O., Perez, B.C., McWhorter, D.E., Cormier, N., Moss, R.F., Johnson, D.J., Neubauer, S.C., Raynie, R.C., 2016. Component greenhouse gas fluxes and radiative balance from two deltaic marshes in Louisiana: Pairing chamber techniques and eddy covariance. J. Geophys. Res. Biogeosciences 121, 1503–1521. https://doi.org/10.1002/2015JG003224.

Li, H., Dai, S., Ouyang, Z., Xie, X., Guo, H., Gu, C., Xiao, X., Ge, Z., Peng, C., Zhao, B., 2018. Multi-scale temporal variation of methane flux and its controls in a subtropical tidal salt marsh in eastern China. Biogeochemistry 137, 163–179. https://doi.org/10.1007/s10533-017-0413-y.

Liu, J., Zhou, Y., Valach, A., Shortt, R., Kasak, K., Kyle, C.R., Dennis, S.H., Derrick, B., 2020. Methane emissions reduce the radiative cooling effect of a subtropical estuarine mangrove wetland by half 4998–5016. doi:10.1111/gcb.15247.

Lu, W., Xiao, J., Liu, F., Zhang, Y., Liu, C., Lin, G., 2017. Contrasting ecosystem CO2fluxes of inland and coastal wetlands: a meta-analysis of eddy covariance data. Glob. Chang. Biol. 23, 1180–1198. https://doi.org/10.1111/gcb.13424.

Macreadie, P.I., Anton, A., Raven, J.A., et al., 2019. The future of Blue Carbon science. Nat Commun 10, 3998. https://doi.org/10.1038/s41467-019-11693-w.

Mäkelä, J., Minunno, F., Aalto, T., Mäkelä, A., Markkanen, T., Peltoniemi, M., 2020. Sensitivity of 21st century simulated ecosystem indicators to model parameters, prescribed climate drivers, RCP scenarios and forest management actions for two Finnish boreal forest sites 2681–2700.

Malone, S.L., Barr, J., Fuentes, JD., Oberbauer, S.F., Staudhammer, C.L., Gaiser, E.E., Starr, G., 2016. Sensitivity to low-temperature events: Implications for CO_2 dynamics in subtropical coastal ecosystems. Wetlands 36, 957–967.

Maricle, B.R., Lee, Æ.R.W., 2007. Root respiration and oxygen flux in salt marsh grasses from different elevational zones 413–423. doi:10.1007/s00227-006-0493-z.

Maricle, B.R., Lee, R.W., 2002. Aerenchyma development and oxygen transport in the estuarine cordgrasses Spartina alterniflora and S. anglica. Aquat. Bot. 74, 109–120. https://doi.org/10.1016/S0304-3770(02)00051-7.

Mauder, M., Foken, T., 2006. Impact of post-field data processing on eddy covariance flux estimates and energy balance closure. Meteologische Zeitschrift 6, 597–609.

McLeod, E., Chmura, G.L., Bouillon, S., Salm, R., Björk, M., Duarte, C.M., Lovelock, C.E., Schlesinger, W.H., Silliman, B.R., 2011. A blueprint for blue carbon: Toward an improved understanding of the role of vegetated coastal habitats in sequestering CO2. Front. Ecol. Environ. 9, 552–560. https://doi.org/10.1890/110004.

McNicol, G., Sturtevant, C.S., Knox, S.H., Dronova, I., Baldocchi, D.D., Silver, W.L., 2017. Effects of seasonality, transport pathway, and spatial structure on greenhouse gas fluxes in a restored wetland. Glob. Chang. Biol. 23, 2768–2782. https://doi.org/10.1111/gcb.13580.

Migliavacca, M., Galvagno, M., Cremonese, E., Rossini, M., Meroni, M., Sonnentag, O., Cogliati, S., Manca, G., Diotri, F., Busetto, L., Cescatti, A., Colombo, R., Fava, F., Morra di Cella, U., Pari, E., Siniscalco, C., Richardson, A.D., 2011. Using digital repeat photography and eddy covariance data to model grassland phenology and photosynthetic CO2 uptake. Agric. For. Meteorol. 151, 1325–1337. https://doi.org/10.1016/j.agrformet.2011.05.012.

Moffett, K.B., Wolf, A., Berry, J.A., Gorelick, S.M., 2010. Salt marsh-atmosphere exchange of energy, water vapor, and carbon dioxide: Effects of tidal flooding and biophysical controls. Water Resour. Res. 46, 1–18. https://doi.org/10.1029/2009WR009041.

Moncrieff, J., Clement, R., Finnigan, J., Meyers, T., 2004. Averaging, detrending and filtering of eddy covariance time series. In: Massman, W J, Law, B E (Eds.), Handbook of micrometeorology: a guide for surface flux measurements. Kluwer Academic, Dordrecht, pp. 7–31.

Moncrieff, J., Massheder, J., De Bruin, H., Elbers, J., Friborg, T., Heusinkveld, B., Kabat, P., Scott, S., Soegaard, H., Verhoef, A., 1997. A system to measure surface fluxes of momentum, sensible heat, water vapour and carbon dioxide. J. Hydrol. 188–189, 589–611.

Morin, T.H., 2019. Advances in the Eddy Covariance Approach to CH 4 Monitoring Over Two and a Half Decades. J. Geophys. Res. Biogeosciences 124, 453–460. https://doi.org/10.1029/2018JG004796.

Morin, T.H., Bohrer, G., Frasson, R.P.D.M., Naor-Azreli, L., Mesi, S., Stefanik, K.C., Schäfer, K.V.R., 2014. Environmental drivers of methane fluxes from an urban temperate wetland park. J. Geophys. Res. G Biogeosciences 119, 2188–2208. https://doi.org/10.1002/2014JG002750.

Negandhi, K., Edwards, G., Kelleway, J.J., Howard, D., Safari, D., Saintilan, N., 2019. Blue carbon potential of coastal wetland restoration varies with inundation and rainfall. Sci. Rep. 1–9. https://doi.org/10.1038/s41598-019-40763-8.

Neubauer, S.C., Franklin, R.B., Berrier, D.J., 2013. Saltwater intrusion into tidal freshwater marshes alters the biogeochemical processing of organic carbon. Biogeosciences 10, 8171–8183. https://doi.org/10.5194/bg-10-8171-2013.

Neubauer, S.C., Megonigal, J.P., 2019. Correction to: Moving Beyond Global Warming Potentials to Quantify the Climatic Role of Ecosystems. Ecosystems 22, 1931–1932. https://doi.org/10.1007/s10021-019-00422-5.

O'Connell, J.L., Alber, A., Pennings, S.C., 2020. Microspatial differences in soil tempereture cause phenology change on par with long-term climate warming in salt marshes. Ecosystems 23, 498–510. https://doi.org/10.1007/s10021-019-00418-1.

Oertel, C., Matschullat, J., Zurba, K., Zimmermann, F., Erasmi, S., 2016. Greenhouse gas emissions from soils—A review. Chemie der Erde - Geochemistry 76, 327–352. https://doi.org/10.1016/j.chemer.2016.04.002.

Petrakis, S., Seyfferth, A., Kan, J., Inamdar, S., Vargas, R., 2017. Influence of experimental extreme water pulses on greenhouse gas emissions from soils. Biogeochemistry 133, 147–164. https://doi.org/10.1007/s10533-017-0320-2.

Peterson, P.M., Romaschenko, K., Arrieta, Y.H., Saarela, J.M., 2014. A molecular phylogeny and new subgeneric classification of Sporobolus (Poaceae: Chloridoideae: Sporobolinae). Taxon 63, 1373–1374.

Piao, S., Yin, G., Tan, J., Cheng, L., Huang, M., Li, Y., Liu, R., Mao, J., Myneni, R.B., Peng, S., Poulter, B., Shi, X., Xiao, Z., Zeng, N., Zeng, Z., Wang, Y., 2015. Detection and attribution of vegetation greening trend in China over the last 30 years. Glob. Chang. Biol. 21, 1601–1609. https://doi.org/10.1111/gcb.12795.

Poffenbarger, H.J., Needelman, B.A., Megonigal, J.P., 2011. Salinity influence on methane emissions from tidal marshes. Wetlands 31, 831–842. https://doi.org/10.1007/s13157-011-0197-0.

Poulter, et al., 2014. variability of the global carbon cycle. Nature 509, 600–603. https://doi.org/10.1038/nature13376.

Rey-Sanchez, A.C., Morin, T.H., Stefanik, K.C., Wrighton, K., Bohrer, G., 2018. Determining total emissions and environmental drivers of methane flux in a Lake Erie estuarine marsh. Ecol. Eng. 114, 7–15. https://doi.org/10.1016/j.ecoleng.2017.06.042.

Richardson, A.D., Braswell, B.H., Hollinger, D.Y., Jenkins, J.P., 2009. Near-surface remote sensing of spatial and temporal variation. Ecol. Appl. 19, 1417–1428. https://doi.org/10.1890/08-2022.1.

Richardson, A.D.A.D.., Black, T.A., Ciais, P., Delbart, N., Friedl, M.A., Gobron, N., Hollinger, D.Y., Kutsch, W.L., Longdoz, B.B.., Luyssaert, S.J., Migliavacca, M.M., Montagnani, L.M., Munger, J.W., Moors, E., Piao, S., Rebmann, C., Reichstein, M., Saigusa, N., Tomelleri, E., Vargas, R., Varlagin, A., 2010. Influence of spring and autumn phenological transitions on forest ecosystem productivity. Philos. Trans. R. Soc. B Biol. Sci. 365, 3227–3246. https://doi.org/10.1098/rstb.2010.0102.

Rosentreter, J.A., Maher, D.T., Erler, D.V., Murray, R.H., Eyre, B.D., 2018. Methane emissions partially offset "blue carbon" burial in mangroves. Sci. Adv. 4 https://doi.org/10.1126/sciadv.aao4985.

Schäfer, K.V.R., Duman, T., Tomasicchio, K., Tripathee, R., Sturtevant, C., 2019. Agricultural and Forest Meteorology Carbon dioxide fluxes of temperate urban wetlands with different restoration history. Agric. For. Meteorol. 275, 223–232. https://doi.org/10.1016/j.agrformet.2019.05.026.

Schäfer, K.V.R., Tripathee, R., Artigas, F., Morin, T.H., Bohrer, G., 2014. Carbon dioxide fluxes of an urban tidal marsh in the Hudson-Raritan estuary. J. Geophys. Res. G Biogeosciences 119, 2065–2081. https://doi.org/10.1002/2014JG002703.

Seyfferth, A.L., Bothfeld, F., Vargas, R., Stuckey, J.W., Wang, J., Kearns, K., Michael, H. A., Guimond, J., Yu, X., Sparks, L., 2020. Spatial and temporal heterogeneity of geochemical controls on carbon cycling in a tidal salt marsh. Geochim. Cosmochim. Acta. 282, 1–18. https://doi.org/10.1016/j.gca.2020.05.013.

Sturtevant, Cove, Oikawa, P.Y., Baldocchi, D., 2016. Identifying scale-emergent, nonlinear, asynchronousprocesses of wetland methane exchange. J. Geophys. Res. Biogeosciences 188–204. https://doi.org/10.1002/2015JG003054.Received.

Tang, J., Körner, C., Muraoka, H., Piao, S., Shen, M., Thackeray, S.J., Yang, X., 2016. SPECIAL FEATURE : INTERNATIONAL LTER Emerging opportunities and challenges in phenology: a review 7, 1–17.

Thompson, B., 1984. Canonical correlation analysis. SAGE, California, USA, pp. 72–pp.

Tokida, T., Miyazaki, T., Mizoguchi, M., Nagata, O., Takakai, F., Kagemoto, A., Hatano, R., 2007. Falling atmospheric pressure as a trigger for methane ebullition from peatland. Global Biogeochem. Cycles 21, 1–8. https://doi.org/10.1029/2006GB002790.

Tonti, N.E., Gassmann, M.I., Pérez, C.F., 2018. First results of energy and mass exchange in a salt marsh on southeastern South America. Agric. For. Meteorol. 263, 59–68. https://doi.org/10.1016/j.agrformet.2018.08.001.

Toomey, M., Friedl, M.A., Frolking, S., Hufkens, K., Klosterman, S., Sonnentag, O., Baldocchi, D.D., Bernacchi, C.J., Biraud, S.C., Bohrer, G., Brzostek, E., Burns, S.P., Coursolle, C., Hollinger, D.Y., Margolis, H.A., McCaughey, H., Monson, R.K., Munger, J.W., Pallardy, S., Phillips, R.P., Torn, M.S., Wharton, S., Zeri, M., Richardson, A.D., 2015. Greenness indices from digital cameras predict the timing and seasonal dynamics of canopy-scale photosynthesis. Ecol. Appl. 25, 99–115. https://doi.org/10.1890/14-0005.1.

Trifunovic, B., Vázquez-Lule, A., Capooci, M., Seyfferth, A.L., Moffat, C., Vargas, R., 2020. Carbon Dioxide and Methane Emissions From a Temperate Salt Marsh Tidal. Journal of Geophysical Research: Biogeosciences 125 (8), 1–16. https://doi.org/10.1029/2019JG005558.

Vasquez, E.D.A. V, Lenn, E.D.P.G., Untenspergen, G.L.R.G., Rown, J.J.E.D.B., Elson, S.T. G.N., 2006. Tolerance and Osmotic Adjustment of S Partina Alterniflora (P Oaceae) and the Invasive M Haplotype of P Hragmites Australis (P Oaceae) Along a Salinity Gradient 193, 1784–1790.

Van de Broek, M., Vandendriessche, C., Poppelmonde, D., Merckx, R., Temmerman, S., Govers, G., 2018. Long-term organic carbon sequestration in tidal marsh sediments is dominated by old-aged allochthonous inputs in a macrotidal estuary. Glob Chang Biol 24 (6), 2498–2512. https://doi.org/10.1111/gcb.14089.

Vázquez-Lule, A., Vargas, R. https://doi.org/10.17190/AMF/1480316.

Vickers, D., Mahrt, L., 1997. Quality Control and Flux Sampling Problems for Tower and Aircraft Data. J. Atmos. Ocean. Technol. 14, 512–526.

Villarreal, S., Guevara, M., Alcaraz-segura, D., Brunsell, N.A., Hayes, D., Loescher, H.W., Vargas, R., 2018. Agricultural and Forest Meteorology Ecosystem functional diversity and the representativeness of environmental networks across the conterminous United States. Agric. For. Meteorol. 262, 423–433. https://doi.org/10.1016/j.agrformet.2018.07.016.

Waldo, N.B., Hunt, B.K., Fadely, E.C., Moran, J.J., Neumann, R.B., 2019. Plant root exudates increase methane emissions through direct and indirect pathways. Biogeochemistry 145, 213–234. https://doi.org/10.1007/s10533-019-00600-6.

Walter, B., Heimann, M., 2000. A process-based, climate-sensitive model to derive methane emissions from natural wetlands : Application to five wetland sites, sensitivity to model parameters, and climate. https://doi.org/10.1029/1999GB001204.

Wang, S.R., Di Iorio, D., Cai, W.-J., Hopkinson, C.S., 2017. Inorganic carbon and oxygen dynamics in a marsh-dominated estuary. Limnol. Oceanogr. 47–71. https://doi.org/10.1002/lno.10614.

Ward, N.D., Megonigal, J.P., Bond-lamberty, B., Bailey, V.L., Butman, D., Canuel, E.A., Diefenderfer, H., Ganju, N.K., Goñi, M.A., Graham, E.B., Hopkinson, C.S., Khangaonkar, T., Langley, J.A., Mcdowell, N.G., Myers-pigg, A.N., Neumann, R.B., Osburn, C.L., Price, R.M., Rowland, J., Sengupta, A., Simard, M., Thornton, P.E., Tzortziou, M., Vargas, R., Weisenhorn, P.B., 2020. Representing the function and sensitivity of coastal interfaces in Earth system models. Nat. Commun. 1–14. https://doi.org/10.1038/s41467-020-16236-2.

Whiting, G.J., Chanton, J.P., 1993. Primary production control of methane emission from wetlands. Nature 364, 794–795. https://doi.org/10.1038/364794a0.

Wutzler, T., Lucas-moffat, A., Migliavacca, M., Knauer, J., Sickel, K., Šigut, L., 2018. Basic and extensible post-processing of eddy covariance flux data with REddyProc 5015–5030.

Zhang, X., Friedl, M.A., Schaaf, C.B., Strahler, A.H., Liu, Z., 2005. Monitoring the response of vegetation phenology to precipitation in Africa by coupling MODIS and TRMM instruments. J. Geophys. Res. D Atmos. 110, 1–14. https://doi.org/10.1029/2004JD005263.

Windham-Myers, L., Bergamaschi, B., Anderson, F., Knox, S., Miller, R., Fujii, R., 2018. Potential for negative emissions of greenhause gases (CO_2, CH_4 and N_2O) through coastal peatland re-establishment: Novel insights from high frequency flux data at meter and kilometer scales. Environmental Research Letters 4. https://doi.org/10.1088/1748-9326/aaae74.

Zhang, Y., Ding, W., 2011. Diel methane emissions in stands of Spartina alterniflora and Suaeda salsa from a coastal salt marsh. Aquat. Bot. 95, 262–267. https://doi.org/10.1016/j.aquabot.2011.08.005.

Zhong, Q., Wang, K., Lai, Q., Zhang, C., Zheng, L., Wang, J., 2016. Carbon Dioxide Fluxes and Their Environmental Control in a Reclaimed Coastal Wetland in the Yangtze Estuary. Estuaries and Coasts 39, 344–362. https://doi.org/10.1007/s12237-015-9997-4.

Kljun, N., Calanca, P., Rotach, M., Schmid, H., 2004 A Simple Parameterisation for Flux Footprint Prediction - Fair-Use Guidelines 2004.

Papale, D., Reichstein, M., Aubinet, M., Canfora, E., Bernhofer, C., Kutsch, W., Longdoz, B., Rambal, S., Valentini, R., Vesala, T., Yakir, D., 2006. Towards a standardized processing of Net Ecosystem Exchange measured with eddy covariance technique: algorithms and uncertainty estimation. Biogeosciences, European Geosciences Union, 2006, 3 (4), pp.571-583.

Lenth, R., Singmann, H., Love, J., Buerkner, P., Herve, M., 2020. Package 'emmeans'. May 25, 2020.